

LIDDICOATITE AND ASSOCIATED SPECIES FROM THE McCOMBE SPODUMENE-SUBTYPE RARE-ELEMENT GRANITIC PEGMATITE, NORTHWESTERN ONTARIO, CANADA

ANDREW G. TINDLE[§]

Department of Earth Sciences, The Open University, Milton Keynes, Buckinghamshire MK7 6AA, U.K.

JULIE B. SELWAY AND FRED W. BREAKS

Ontario Geological Survey, Precambrian Geoscience Section, 933 Ramsey Lake Road, Sudbury, Ontario P3E 6B5, Canada

ABSTRACT

Liddicoatite, a rare species of tourmaline, has been found in the McCombe pegmatite, of complex type and spodumene subtype, an example of the LCT (lithium, cesium, tantalum) family. It is one of a group of beryl- and complex-type pegmatites exposed along the Uchi – English River subprovincial boundary-zone, Ontario, in the Superior Province of the Canadian Shield. The mineral assemblage containing zoned “fluor-elbaite”–liddicoatite crystals was the last product of primary, near-solidus crystallization of the pegmatite and is unique not only to this subprovincial boundary, but also throughout the vast number of rare-element pegmatites distributed across Ontario. The most calcic composition of liddicoatite analyzed here corresponds to $(\text{Ca}_{0.5}\text{Na}_{0.4}\square_{0.1}) (\text{Li}_{1.5}\text{Al}_{1.2}\text{Mn}_{0.2}\text{Fe}_{0.1}) \text{Al}_6(\text{Si}_6\text{O}_{18}) (\text{BO}_3)_3 (\text{OH}_{3.4}\text{F}_{0.6})$. Other calcium-enriched species found in the McCombe pegmatite include microlite $(\text{Ca}_{1.2}\text{Na}_{0.6}\square_{0.2})(\text{Ta}_{1.6}\text{Nb}_{0.3}\text{Sn}_{0.1})\text{O}_6(\text{F}_{0.7}\text{OH}_{0.3})$, Ca-enriched almandine $(\text{Alm}_{44.6}\text{Sps}_{26.4}\text{Grs}_{26.2})$, Ca-enriched spessartine $(\text{Sps}_{69.3}\text{Alm}_{19.8}\text{Grs}_{10.9})$, and fluorapatite. Evidence from progressively evolved units of the pegmatite and mineral zonation shows that contamination of the pegmatite-forming melt occurred, and that fluids from the pegmatite migrated out into the mafic metavolcanic host-rocks, creating a Li-, Cs-, and B-enriched metasomatic aureole. The evolution of the pegmatite-forming melt resulted in increased activity of fluorine, and the essentially *in situ* fractionation of the contaminated melt led to the crystallization of the rare-element-enriched minerals. Patterns of zonation seen in back-scattered-electron images show that primary crystallization of columbite–tantalite, garnet and tourmaline species involved multiple episodes of growth and dissolution in a dynamic system. Liddicoatite was able to form, not because of any one of these processes, but because they all acted together to concentrate both Li and Ca, a sequence of events that is apparently very rare in nature.

Keywords: tourmaline, liddicoatite, elbaite, rare element, lithium, tantalum, cesium, granitic pegmatite, host-rock interaction, contamination, Ontario, Canada.

SOMMAIRE

Nous avons trouvé la liddicoatite, une espèce rare de tourmaline, dans la pegmatite granitique de McCombe, exemple d'une pegmatite de type LCT (à lithium, césium, tantale) de type complexe et de sous-type à spodumène. C'est une pegmatite d'un groupe à béryl et de type complexe affleurant le long de la frontière entre les sous-provinces de Uchi et de English River en Ontario, dans la Province du Supérieur du Bouclier Canadien. L'assemblage de minéraux contenant les cristaux zonés de “fluor-elbaite”–liddicoatite était l'ultime produit de cristallisation primaire, près du solidus du magma; l'assemblage est unique non seulement le long de cette frontière entre sous-provinces, mais aussi parmi le vaste ensemble de pegmatites enrichies en éléments rares distribuées partout en Ontario. La composition la plus calcique de liddicoatite analysée correspond à $(\text{Ca}_{0.5}\text{Na}_{0.4}\square_{0.1}) (\text{Li}_{1.5}\text{Al}_{1.2}\text{Mn}_{0.2}\text{Fe}_{0.1}) \text{Al}_6(\text{Si}_6\text{O}_{18}) (\text{BO}_3)_3 (\text{OH}_{3.4}\text{F}_{0.6})$. Parmi les autres espèces enrichies en calcium dans la pegmatite de McCombe se trouvent la microlite $(\text{Ca}_{1.2}\text{Na}_{0.6}\square_{0.2})(\text{Ta}_{1.6}\text{Nb}_{0.3}\text{Sn}_{0.1})\text{O}_6(\text{F}_{0.7}\text{OH}_{0.3})$, l'almandine calcifère $(\text{Alm}_{44.6}\text{Sps}_{26.4}\text{Grs}_{26.2})$, la spessartine calcifère $(\text{Sps}_{69.3}\text{Alm}_{19.8}\text{Grs}_{10.9})$, et la fluorapatite. D'après l'évidence venant des unités progressivement plus évoluées de la pegmatite et de la zonation des minéraux, une contamination du liquide formateur de la pegmatite s'est produite, et les fluides émanant de la pegmatite ont migré vers l'extérieur, pour former une auréole métasomatique enrichie en Li, Cs, et B dans l'encastement mafique métavolcanique. L'évolution continue du liquide granitique contaminé a mené à une activité accrue du fluor, et à une cristallisation *in situ* des minéraux enrichis en éléments rares. Les tracés de zonation révélés par les images des électrons rétrodiffusés montrent que la cristallisation primaire de la columbite–tantale, du grenat et des espèces de tourmaline a impliqué de multiples épisodes de croissance et de dissolution dans un système dynamique. La liddicoatite a pu se former, non à cause d'un

[§] E-mail address: a.g.tindle@open.ac.uk

seul de ces processus, mais parce qu'ils ont agi ensemble pour concentrer à la fois le Li et le Ca, séquence d'événements qui semble très inhabituelle dans la nature.

(Traduit par la Rédaction)

Mots-clés: tourmaline, liddicoatite, elbaïte, élément rare, lithium, tantale, césium, pegmatite granitique, interaction avec l'encaissant, contamination, Ontario, Canada.

INTRODUCTION

Liddicoatite has only been found in abundance at the type locality and its analogues in Madagascar (Dunn *et al.* 1977, Aurisicchio *et al.* 1999, Akizuki *et al.* 2001, Dirlam *et al.* 2002). So unusual is it that Teertstra *et al.* (1999a) referred to it as the "stranger in paradise" in describing its occurrence in the High Grade Dyke, a spodumene-subtype pegmatite in southeastern Manitoba, Canada. The High Grade Dyke is a member of the Cat Lake – Winnipeg River pegmatite field, belonging to the Maskwa Lake pegmatite series, and outcrops mainly in the Bird River Greenstone Belt, close to the English River Subprovince. Interestingly, 330 km to the east of this pegmatite but within a different subprovince, is the McCombe pegmatite, the subject of this paper. The only other examples of liddicoatite reported worldwide are from Mozambique (Sahama *et al.* 1979), Malkhan, Russia (Zagorskyi *et al.* 1989), the Czech Republic (Novák & Povondra, 1995, Novák & Selway 1997, unpubl. data of J.B. Selway), Nigeria, Tanzania and Vietnam (Dirlam *et al.* 2002) and Minas Gerais, Brazil (Bastos 2002, Dirlam *et al.* 2002). As a further example of the rarity of liddicoatite, only one of over 300 tourmaline-bearing samples examined by the authors from a wide range of Ontarian rare-element pegmatites and their host rocks contains liddicoatite.

Liddicoatite is so rare because it contains substantial amounts of the elements Li and Ca. In the normal sequence of events, these elements are decoupled during Li-enriched pegmatite formation. Typically, Ca enters minerals in early-crystallizing endocontact and border- to wall-zone assemblages (*e.g.*, feldspar and fluorapatite), whereas Li is concentrated in relatively late-crystallizing phases such as Li-aluminosilicates (spodumene or petalite) and lepidolite (Černý 1991).

At the type locality in Madagascar, liddicoatite formed because the pegmatite-forming melt was contaminated with marble host-rocks (Dunn *et al.* 1977), whereas in Manitoba, Teertstra *et al.* (1999a) argued that there was no influx of Ca into the pegmatite-forming melt and suggested instead that Ca in the High Grade Dyke could have been residual from the original bulk-composition of the pegmatite. Interestingly, a similar disparate set of views has been expressed for the origin of elbaite-subtype pegmatites, as the Vlastějovice pegmatite in the Czech Republic is considered to be contaminated by host rocks (Novák & Povondra 1995),

whereas the O'Grady batholith in the Northwest Territories of Canada contains elbaite-subtype pegmatites interpreted to be fractionated from a hornblende granite (Ercit *et al.* 2003).

It is our purpose in this paper to examine these conflicting models in the light of evidence from the McCombe pegmatite.

GEOLOGICAL SETTING OF THE MCCOMBE PEGMATITE

The McCombe pegmatite is one of a number of rare-element pegmatites that occur over a 350 km strike-length of the boundary zone between the Uchi and the English River subprovinces, in the Superior Province of Ontario (Figs. 1a–c). The belt of pegmatites begins in the west with the Sandy Creek beryl-type pegmatite in the Ear Falls area and extend eastward to the Lilypad Lake complex-type, spodumene-subtype pegmatite in the Fort Hope area (Wallace 1978, Teertstra *et al.* 1999b). Rare-element mineralization is known in three intervening areas, with beryl-type pegmatites at Jubilee Lake and spodumene-subtype pegmatites at both Root Lake and East Pashkokogan Lake (Breaks *et al.* 2001).

Fertile peraluminous granites that generated rare-element mineralization in this boundary zone have thus far been postulated for the Sandy Creek pegmatite (Wenasaga Lake batholith) and the Jubilee Lake pegmatite group (Allison Lake batholith; Fig. 1c). The Root Lake group of pegmatites (consisting of the Consolidated Morrison and the larger McCombe pegmatites) is also tentatively linked to the Allison Lake batholith, which has its most chemically evolved region in the southeast, nearest these pegmatites (Fig. 1c; Breaks *et al.* 2003).

The McCombe pegmatite, consisting of two main dykes, was discovered in 1956 during an exploration boom for lithium (Pye 1956). The dykes were traced on surface for a strike length of 550 m, and diamond drilling (55 holes totaling 10,442 m) established 2.297 million tonnes grading 1.3% Li₂O (Mulligan 1965, p. 64). The best exposure of these pegmatite dykes, situated toward the western end, has been mapped and described by Breaks & Bond (1993). Dyke 1 is the larger and is intermittently exposed for a strike length of 176 m, with a maximum width of 15 m. Dyke 2 is lens-shaped in plan and measures 87 by 19 m.

Five internal divisions have been mapped in the two McCombe dykes, although only the spodumene zone is

of significant areal extent (Fig. 1d). 1) The tourmalinite unit consists of massive tourmalinite that formed along the contact with host rocks and the tourmaline–plagioclase-rich wall zone of Dyke 1. According to its localized distribution and proximity to the pegmatite contact, we suggest that it represents heavily modified host-rocks rather than being a magmatic zone of the pegmatite. In places, tourmaline concentrations are interlayered with thin garnet-rich horizons. Muscovite and epidote also are present. 2) The wall zone, a tourmaline–plagioclase-rich pegmatite, consists of a thin, discontinuous zone, best developed along the southern margin of Dyke 1 and, to a lesser extent, along the northern margin of Dyke 2. There is some evidence that this is a contaminated unit, as it contains minor calcite and biotite–tourmaline-rich clots that likely represent fragments of partially digested host-rocks (selvedge). Minor garnet, rare arsenopyrite and löllingite are present. 3) The spodumene zone, porphyritic with either a pegmatitic matrix or an aplitic matrix, tourmaline-bearing and K-feldspar-phyric, developed in both dykes, but the matrix is particularly pegmatitic in Dyke 1 and aplitic

in Dyke 2. This zone is characterized by white coarse-grained porphyritic K-feldspar and prismatic beige, white and green spodumene up to 8 cm long in the pegmatitic matrix. 4) The aplite unit is tourmaline-bearing, equigranular and K-feldspar-phyric, developed very locally in parts of the spodumene zone of Dyke 2. This zone contains orange-red garnet, muscovite and lenticular quartz, which makes the aplite seem foliated. Spatially, this unit and the lepidolite unit represent a very minor component of the pegmatite and are therefore referred to as a (minor) unit rather than a zone. 5) The lepidolite unit consists of pods and seams that have formed in close proximity to the tourmalinite unit of Dyke 1, but within the spodumene zone. The volumetrically minor lepidolite unit is not, however, insignificant, as it appears to be the most evolved part of the pegmatite. It contains beige prismatic spodumene intergrown with quartz.

The McCombe pegmatite intrudes massive and pillowed mafic metavolcanic rocks with lenses of biotite metawacke of the Lake St. Joseph greenstone belt within the Uchi Subprovince. The mafic metavolcanic

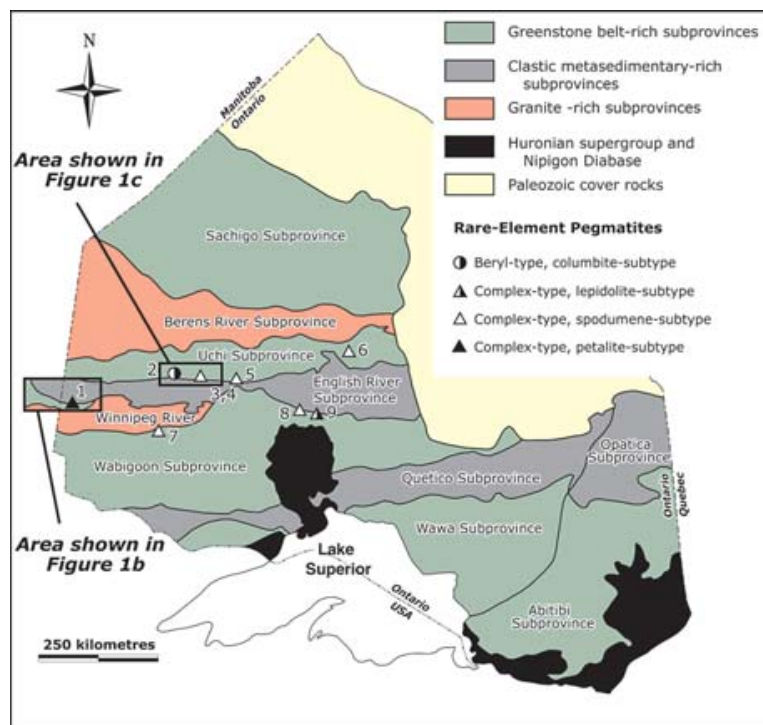


FIG. 1a. Map of the Superior Province showing Ontario pegmatites mentioned in the text. 1 Separation and southeastern Manitoba pegmatites, 2 Sandy Creek pegmatite, 3 McCombe pegmatite, 4 Consolidated Morrison pegmatite, 5 East Pashkokogan pegmatite, 6 Lilypad Lake pegmatite, 7 Dryden pegmatites (includes Tot Lake), 8 Falcon Lake, 9 Swole Lake.

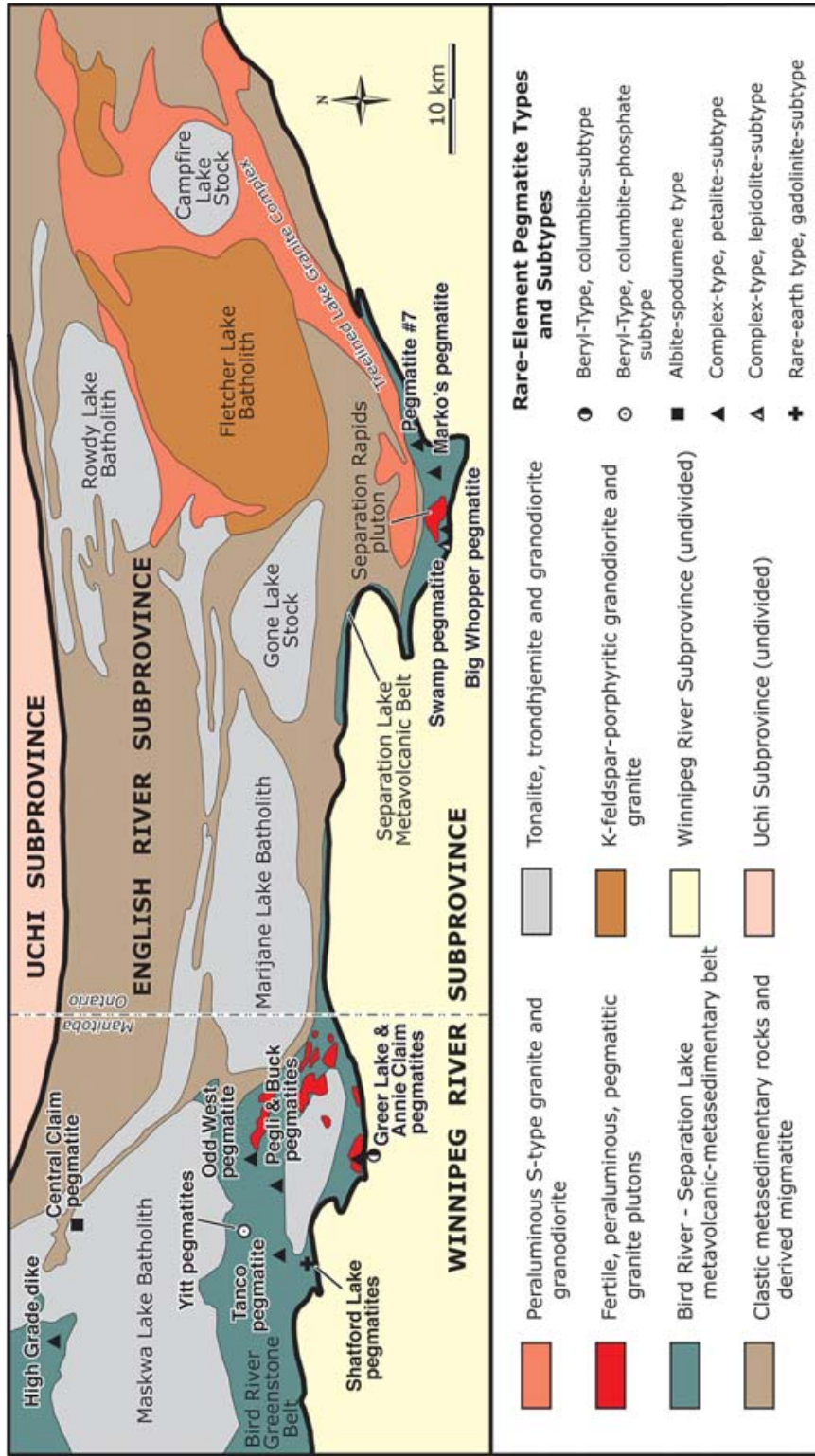


FIG. 1b. Map showing the distribution of pegmatite bodies close to the Ontario-Manitoba border, predominantly within the English River Subprovince, Separation Lake metavolcanic belt, and Bird River metavolcanic-metasedimentary belt. Compiled from Čorný *et al.* (1981) and Breaks & Bond (1993).

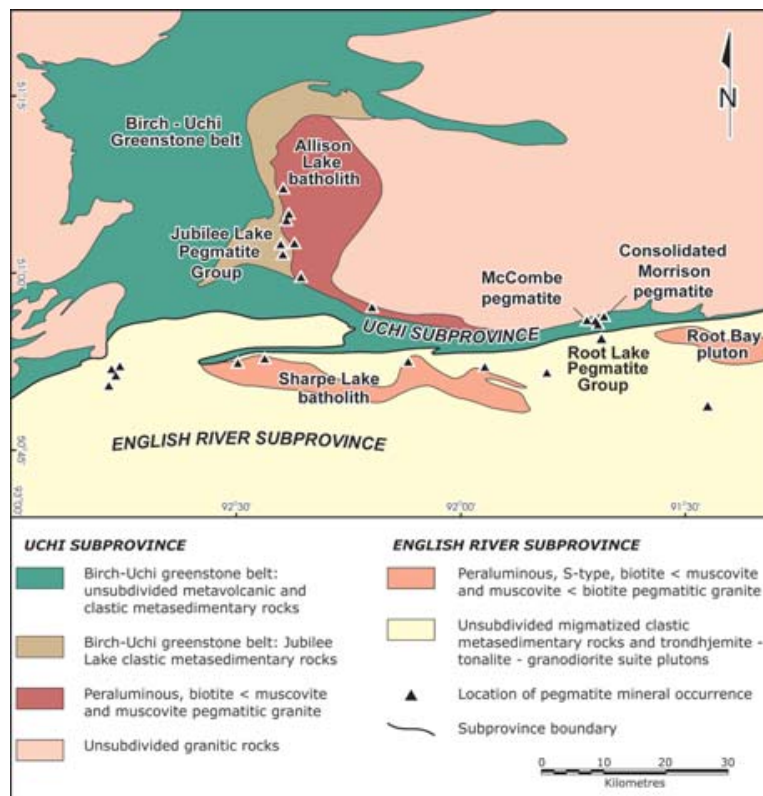


FIG. 1c. Map showing the location of important bodies of granitic pegmatite along the English River and Uchi Subprovince boundaries and associated with the Allison Lake batholith. Compiled from Thurston *et al.* (1985a, b), Breaks & Bond (1993) and Breaks *et al.* (2001).

rocks have been metamorphosed to the amphibolite facies. Unaltered, massive, fine-grained green amphibolite is hornblende-rich (magnesian hornblende) with common epidote, calcite, prismatic Carlsbad-twinned plagioclase and minor pyrite, chalcopyrite, titanite. The amphibolite is cross-cut by numerous veins of calcite. The abundance of calcite in the amphibolite is reflected by the elevated Ca and CO₂ contents (14.71 wt.% CaO, 1.33 wt.% CO₂) in bulk whole-rock compositions.

Closest to the pegmatite, metasomatized host-rocks consists of abundant biotite and tourmaline with minor holmquistite, hornblende and garnet. The metasomatic biotite is a (Rb,Cs)-rich siderophyllite (Breaks *et al.* 2003). Slightly further away from the pegmatite contact, the metasomatized host-rock is strongly foliated and consists of abundant, fibrous, purple holmquistite, minor hornblende and plates of biotite that wrap around garnet porphyroblasts. Bulk whole-rock compositions indicate depletion in Ca (4.78 wt.% CaO) and CO₂ (0.35 wt.% CO₂) relative to unaltered amphibolite, although the holmquistite aureole contains several calc-silicate

accessory minerals: plagioclase, epidote and titanite. The holmquistite aureole also contains localized areas with approximately 20% of white armenite (BaCa₂Al₆Si₉O₃₀•2H₂O) (Breaks *et al.* 2001, 2003). Elsewhere, armenite is a species typically found in interbedded mafic calc-silicates and pyritiferous graphitic schists derived from dolomitic marls, as at Loch Kander, in the Grampian Region of Scotland (Fortey *et al.* 1991, 1993).

The presence of an inner biotite + tourmaline aureole and an outer holmquistite-rich aureole indicates that (Rb, Cs, B, Al, Li)-rich fluids migrated from the pegmatite into the amphibolite host-rock. At the same time, Ca and CO₂ were depleted in the aureole rocks as hornblende was replaced with holmquistite. Assuming that some (if not all) of the calcite in the unaltered amphibolite existed prior to the intrusion of the McCombe pegmatite, then its absence in the aureole rocks indicates further loss of Ca and CO₂ during the metasomatic process.

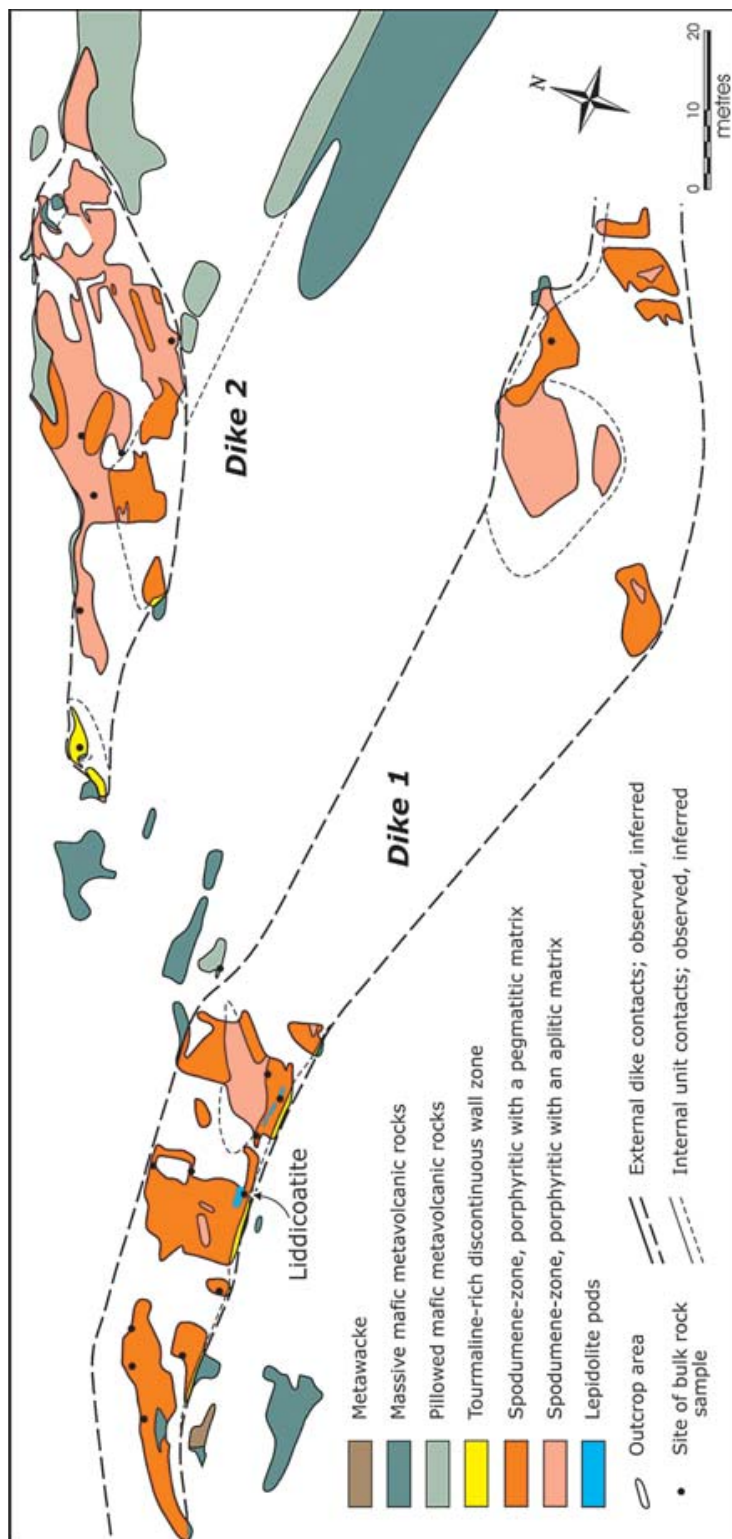


Fig. 1d. Map of the McCombe pegmatite. Note that the very localized aplitic unit is not shown on this figure. Blue dots represent those samples containing lepidolite. The map is derived from Breaks & Bond (1993).

Although mafic metavolcanic rocks appear to be the dominant host-rock to the McCombe pegmatite, there are isolated outcrops of an unaltered, foliated, fine-grained biotite metawacke consisting of abundant granoblastic quartz, platy aligned biotite and minor plagioclase. Close to the contact, the metawacke to the east and west of Dyke 1 contains accessory muscovite and rare apatite, locally accompanied by plagioclase, hornblende, biotite, ilmenite and epidote. A bulk whole-rock composition indicates 6.51 wt.% CaO for one such sample.

EXPERIMENTAL METHODS

Mineral analyses were made in the Department of Earth Sciences at the Open University with a Cameca SX100 electron microprobe operating in wavelength-dispersion mode. The following standards and X-ray lines were used: synthetic LiF (FK α), jadeite (NaK α), forsterite (MgK α), K-feldspar (AlK α , SiK α , KK α), synthetic KCl (ClK α), rutile (TiK α), bustamite (MnK α , CaK α), hematite (FeK α), willemite (ZnK α), Nb metal (NbL α), Ta metal (TaL α), cassiterite (SnL α), synthetic WO₃ (WL α), crocoite (PbM α), synthetic ThO₂ (ThM α), synthetic UO₂ (UM β), synthetic ScPO₄ (ScK β), Bi₂Se₃ (BiM α) and stibnite (SbL α). An operating voltage of 20 kV and probe current of 20 nA (measured on a Faraday cage) were used, with a beam 10 μ m in diameter. Count times varied from 20 to 80 seconds per element, and data were corrected using a PAP correction procedure (Pouchou & Pichoir 1985).

The chemical formula of tourmaline $XY_3Z_6[T_6O_{18}][BO_3]_3V_3W$ and the nomenclature used here follow the recommendations of Hawthorne & Henry (1999), where X represents Ca, Na, \square ; $Y = \text{Li, Mg, Fe}^{2+}, \text{Mn}^{2+}, \text{Al, Zn, Fe}^{3+}, \text{Ti}^{4+}$; $Z = \text{Mg, Al, Fe}^{3+}$; $T = \text{Si, Al}$; $B = \text{B}$; $V = \text{OH, O}$; $W = \text{OH, F, O}$. The species "fluor-elbaite", "manganofoitite", "oxy-manganofoitite", "oxy-liddicoatite" and "hydroxy-liddicoatite" have not been formally described, and are not yet IMA-sanctioned. They are theoretical end-members identified by Hawthorne & Henry (1999). Other tourmaline-group species mentioned in this paper include uvite, foitite, schorl, elbaite, rossmanite and liddicoatite.

Structural formulae were calculated on the basis of 31 anions, assuming stoichiometric amounts of H₂O as (OH), *i.e.*, OH + F = 4 *apfu* (atoms per formula unit), B₂O₃ (B = 3 *apfu*) and Li₂O (as Li⁺) (Burns *et al.* 1994, MacDonald *et al.* 1993). The amount of Li assigned to the Y site corresponds to the ideal sum of the $T + Z + Y$ cations (15 *apfu*) minus the sum of the cations actually occupying these sites [$\text{Li} = 15 - (T + Z + Y)$ or $\text{Li} = 15 - (\text{Si} + \text{Al} + \text{Mg} + \text{Fe} + \text{Mn} + \text{Zn} + \text{Ti})$]; the calculation was iterated to self-consistency. All Fe and Mn were assumed to be divalent. We were unable to estimate the amount of Fe³⁺ or O²⁻ (substitution for OH).

A Microsoft Excel™ worksheet was used to perform structural-formula calculations of tourmaline and is

available from the following web address: <http://www.open.ac.uk/earth-research/tindle>

COMPOSITION OF THE MINERALS

An extensive electron-microprobe investigation of various minerals from the McCombe pegmatite dykes has revealed a highly evolved rare-element system dominated by spodumene, (Rb-Cs)-rich K-feldspar and a (Nb-Ta)-rich oxide assemblage of manganocolumbite, manganotantalite, and microlite, occurring with minor petalite, Cs-rich beryl, Rb- and Cs-rich lepidolite, garnet (almandine–spessartine), fluorapatite, schorl, elbaite, "fluor-elbaite" and liddicoatite, the latter representing the most evolved lithium-bearing tourmaline composition yet described in the Superior Province of Ontario. These data are here described and compared with other rare-element pegmatites from the Superior Province of Canada.

K-feldspar

Rb- and Cs-bearing K-feldspar has been analyzed from three of the zones in the McCombe pegmatite (Fig. 2a). Average Rb and Cs contents increase from the spodumene zone to the aplite unit and increase further in the lepidolite unit (1.56 \Rightarrow 1.84 \Rightarrow 2.07 wt.% Rb₂O and 0.09 \Rightarrow 0.14 \Rightarrow 0.29 wt.% Cs₂O, respectively). The elevated values are similar to those in (Rb,Cs)-bearing K-feldspar from Tanco (Tanco pegmatite, Lac du Bonnet, Manitoba; A.G. Tindle, unpubl. data). In Ontario, only feldspar from Pegmatite 7 (one of the Separation Rapids pegmatites), Lilypad Lake and Falcon Lake pegmatites contain appreciably higher rare-element contents (Fig. 2a). Clearly, in the McCombe pegmatite, the magma was able to fractionate so that rare elements attained a greater degree of enrichment than most other pegmatites in the Superior Province (including many not shown on Fig. 2a; Breaks *et al.* 2003), but it does not appear to have been aided by P-fluxing, as phosphorus contents of the K-feldspar are relatively low (averaging 0.02 wt.% P₂O₅). This is in sharp contrast to certain other petalite- and spodumene-subtype pegmatites in the Superior Province, where the P content of (Rb,Cs)-enriched K-feldspar is much higher (*e.g.*, at Lilypad Lake, 0.14%, at Tanco, 0.40%, at Swole Lake, 0.41%, at East Pashkokogan, 0.62%, at Swamp (Separation Rapids), 0.72%, and at Falcon Lake, 0.80 wt.% P₂O₅).

Columbite-group minerals

Much of the Ta in the McCombe pegmatite is held in euhedral crystals of manganocolumbite, which generally exhibit progressive or oscillatory zonation. Figure 3a shows manganocolumbite from the spodumene zone that crystallized with subtle progressive zonation in the core region, followed by crystallization of a porous (fluid-inclusion-rich?) zone, again progressively zoned. A period of dissolution followed before crystal-

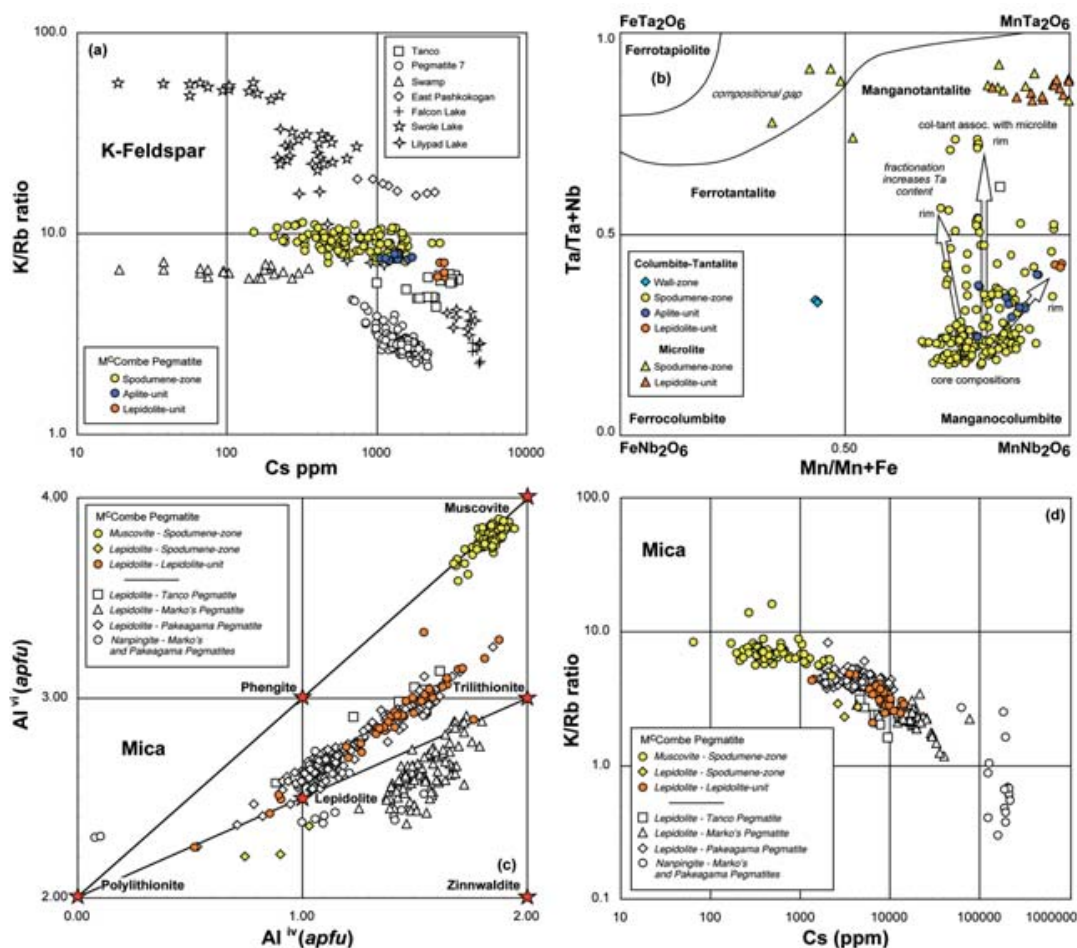


FIG. 2. (a) Covariation of K/Rb *versus* Cs in K-feldspar of the McCombe pegmatite and other evolved pegmatites from the Superior Province. (b) Composition of columbite–tantalite from the McCombe pegmatite plotted in terms of the columbite–tantalite quadrilateral. The location of the compositional gap is based on results of 7400 analyses of ferrotapiolite and columbite–tantalite from rare-element pegmatites of Ontario. For convenience, data on microlite are also plotted on this diagram. The white square is the average of columbite–tantalite data from Tanco (Černý *et al.* 1998). (c) Covariation of ^{IV}Al *versus* ^{VI}Al in micas. (d) Covariation of Cs *versus* K/Rb in micas. The structural formulae of the micas were calculated using the method of Tindle & Webb (1990). Data on the Tanco pegmatite were taken from Rinaldi *et al.* (1972), Černý & Macek (1972), Černý *et al.* (1998) & Teertstra *et al.* (1998). The remaining data were mainly published in Tindle *et al.* (2001) and Tindle *et al.* (2002a). Pegmatite 7, Swamp Pegmatite and Marko's Pegmatite are all from the Separation Lake area of north-western Ontario.

lization began again, leaving behind a succession of fluctuating thin oscillatory zones. Throughout this sequence, Ta varied from 36 to 43 wt.% Ta₂O₅, a relatively modest change in composition. In a few samples, there is a progressive increase of Ta from core to rim of individual crystals, such that compositions fall in the manganotantalite field (Fig. 2b), and Ta contents there approach 70 wt.% Ta₂O₅. There does not appear to have been a great increase in Ta between zones, as averages

within the spodumene zone and the aplite unit are 31.7 and 35.9 wt.% Ta₂O₅, respectively; although the dataset consists of nearly 200 analyses from over 20 samples, these figures may not be particularly representative because of the amount of zonation (and hence variable composition) observed. One small crystal of ferrocolumbite was identified in a wall-zone sample, consistent with this being an early-crystallizing zone, but data are too sparse to be interpreted more fully.

Unlike other pegmatites, such as the North Aubry pegmatite, a spodumene-subtype pegmatite in the Wabigoon Subprovince (Breaks *et al.* 2001, 2003), the melt did not continue to be enriched in Ta in the McCombe pegmatite, to produce extreme (end-member) manganotantalite compositions, but instead formed microlite. Microlite is not a widespread or common species, and is only reported from the spodumene zone and lepidolite unit, where it formed isolated crystals or thin veinlets, such as those illustrated in Figure 3a. Paragenetically, microlite most likely formed during protracted fractionation of the pegmatite-forming melt and after much of the pegmatite had solidified. The result is either primary grains of microlite [Mn/(Mn + Fe) averaging 0.92], especially in the lepidolite unit, or a mantle of microlite [Mn/(Mn + Fe) averaging 0.43] replacing earlier-formed columbite–tantanite. The main importance of microlite, however, is that it is both a Ca- and F-rich species, and that it formed late in the evolution of the pegmatite, both significant characteristics in our efforts to understand the formation of liddicoatite.

Micas

Rare-element enrichment also is found in micas from the McCombe pegmatite. Muscovite is the most common species (Fig. 2c). In the spodumene zone, it forms anhedral primary crystals averaging 1.33 wt.% Rb₂O and 0.07 wt.% Cs₂O. In a few samples, the margin of muscovite crystals has been replaced by minerals of the lepidolite series, whose greatly increased rare-element content (averaging 2.63 wt.% Rb₂O and 0.58 wt.% Cs₂O), indicates late enrichment and mobility of these elements in late-magmatic fluids. Further enrichment occurs in the lepidolite unit, where in massive lepidolite pods and seams, the lepidolite-series minerals average 2.77 wt.% Rb₂O and 0.95 wt.% Cs₂O, and compositions approach the (Li–F)-rich end-member, polyolithionite (KLi₂AlSi₄O₁₀F₂) (Fig. 2c). For Cs, this enrichment is more extreme than that reported at Tanco (average 3.39 wt.% Rb₂O, 0.70 wt.% Cs₂O; Rinaldi *et al.* 1972, Černý *et al.* 1998). Greater enrichment of Cs in mica is, however, reported from other pegmatites in the region (Fig. 2d), notably at Separation Lake (Marko's pegmatite) and

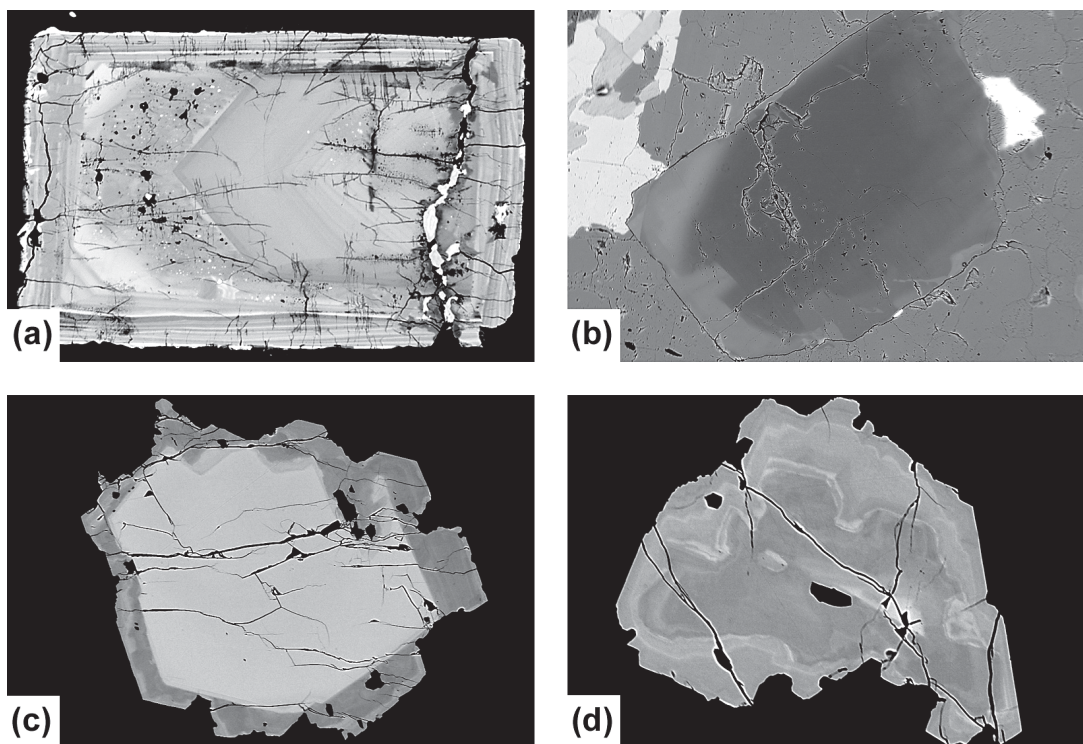


FIG. 3. Back-scattered-electron (BSE) images. (a) Euhedral crystal of manganocolumbite showing multiple episodes of crystallization, resorption and late veining by microlite in spodumene-zone sample RR8 (width of field of view 620 μm). (b) Beryl with irregular Cs-rich rim in spodumene-zone sample RR17 (width of field of view 1700 μm). (c) Garnet with Ca-rich overgrowth in wall-zone sample RR32B (width of field of view 950 μm). (d) Irregularly shaped grain of garnet with a complex pattern of zonation in which enrichment in Ca is pervasive; wall-zone sample RR32B (width of field of view 450 μm).

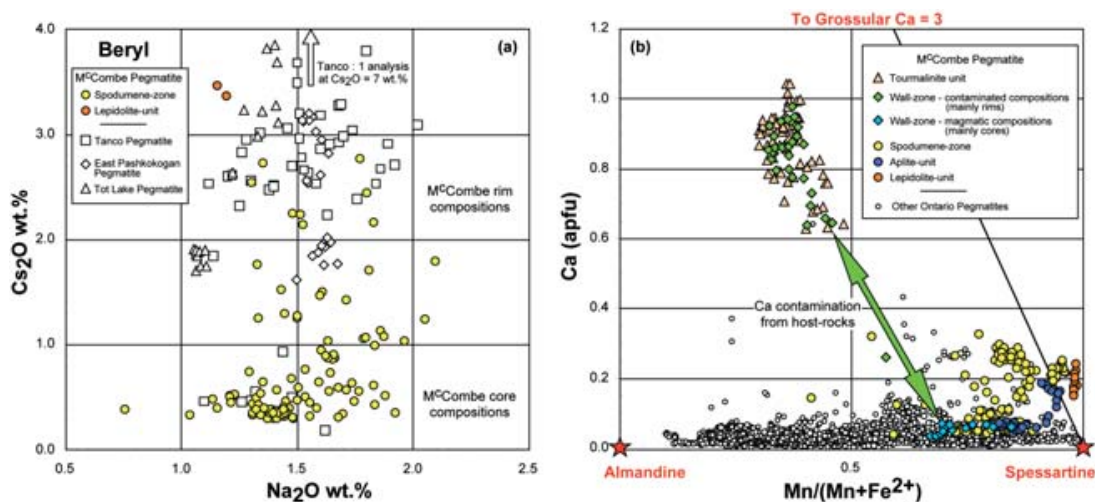


FIG. 4. (a) Covariation of Na versus Cs in beryl; oxide data are plotted here as some analyses are incomplete, and structural formulae could not be calculated. Beryl data from Tanco and other pegmatites are from Černý & Simpson (1977), Burt (1982), Černý *et al.* (1998), and Tindle *et al.* (2002a). (b) Covariation of Mn/(Mn + Fe²⁺) versus Ca in garnet. Other data (1300 analyses) on garnet from Ontario pegmatites are from Tindle *et al.* (2002a) or unpublished.

Pakeagama Lake, where nanpingite, with up to 23.07 wt.% Cs₂O, is (rarely) found (Breaks & Tindle 2002; A.G. Tindle, unpubl. data). As there is no muscovite in the lepidolite unit of the McCombe pegmatite, the lepidolite could be primary, but the possibility also exists that it may have totally replaced earlier muscovite. The occurrence of lepidolite-series minerals in pods and seams suggests that these may have crystallized from trapped pockets of residual fluid or hydrous melt within the mostly consolidated pegmatite.

Further evidence for movement of rare elements in a fluid phase is provided by the host rocks adjacent to the pegmatite. Close to the pegmatite contact, mafic metavolcanic rocks have been metasomatically altered to a variable assemblage of holmquistite, magnesiohornblende, tourmaline, biotite, fluorapatite, epidote, titanite and quartz. The biotite has a composition close to siderophyllite, but with a rare-element content averaging 1.53 wt.% Rb₂O and 1.12 wt.% Cs₂O. This enrichment could only have occurred by the escape of evolved fluids from the pegmatite, thus confirming migration of rare elements into the host rocks. During this event, whole-rock Rb contents increased from 5–17 ppm Rb in unaltered host-rocks to 116–324 ppm Rb in metasomatized holmquistite-bearing host-rocks adjacent to the pegmatite.

Beryl

There is some evidence to suggest that Cs also was concentrated in beryl in a similar way to that in mica. Beryl is a commonly encountered accessory mineral in

the spodumene zone of the McCombe pegmatite, where it forms euhedral to subhedral crystals typically with a Cs content of 0.5 wt.% Cs₂O. In a few cases, this primary composition has been modified (replaced) around the margins of crystals by later Cs-rich fluids that have raised Cs contents up to 2.76 wt.% (Figs. 3b, 4a). This composition is comparable to beryl from Tanco (average 2.56 wt.% Cs₂O; Černý & Simpson 1977, Burt 1982, Černý *et al.* 1998) and a few other Ontario pegmatites (*e.g.*, Tot Lake; average 2.50 wt.% Cs₂O and East Pashkokogan; average 2.45 wt.% Cs₂O; Tindle *et al.* 2002a).

Garnet

The chemical composition of garnet in the pegmatite is restricted to the almandine–spessartine series, with variable, but generally minor, Mg and Ca contents (Černý & Hawthorne 1982). In Figure 4b, we illustrate this pattern of variation and compare garnet from the McCombe pegmatite with that from other Ontario pegmatites (Breaks *et al.* 2003; A.G. Tindle, unpubl. data).

Garnet compositions from the wall zone, spodumene zone and aplite unit of the McCombe pegmatite (Table 1) become progressively Mn-rich, and approach the end-member composition of spessartine in the lepidolite unit, where Mn/(Mn + Fe²⁺) = 0.99 (equivalent to Sps_{93.8}Grs_{4.3}Alm_{1.2}Adr_{0.7}). Garnet from the lepidolite unit also has a minor F content, up to 0.23 wt.%, and is comparable to that noted by Teertstra *et al.* (1999a) in the High Grade Dyke, Manitoba.

Analytical traverses across zoned crystals of garnet from the McCombe pegmatite show that Ca also is enriched toward the rim of crystals. In the wall zone, two types of garnet are found; (i) those with Ca-poor spessartine cores (Ca = 0.06 *apfu*) and marked Ca-rich almandine overgrowths ($0.78 < \text{Ca} < 1.04$ *apfu* or equivalent to 25–33% of the grossular component), in which there appears to have been a rapid change in conditions of crystallization and at which time appreciably more Ca became available to the pegmatite-forming melt (Fig. 3c); (ii) more irregularly shaped grains with complex patterns of zonation (Fig. 3d) in which Ca-enrichment is pervasive (0.65–0.92 *apfu* Ca, or equivalent to 21–29% of the grossular component). The irregular patterns suggest that disequilibrium conditions prevailed.

In the tourmalinite unit, localized concentrations of garnet are interlayered with more tourmaline-rich regions and have identical Ca-rich almandine compositions (0.63–1.04 *apfu* Ca) to the overgrowths in the wall-zone samples (Fig. 4b). We have already suggested that the tourmalinite unit may represent selvage derived from host rocks. We further suggest that part of this leaching or digestion process was the liberation of Ca into the pegmatite-forming melt to produce localized disequilibrium in the wall zone, because the pegmatite-forming melt cooled too rapidly for equilibrium to be attained.

Surprisingly, even though garnet crystals in samples from the inner zones of the pegmatite do not show any textures indicative of obvious disequilibrium or other indications of contamination, they too have significant grossular components. Relative to the majority of other

TABLE 1. COMPOSITION OF GARNET FROM THE MCCOMBE GRANITIC PEGMATITE, NORTHWESTERN ONTARIO

	Tourmalinite Unit		Wall Zone			Spodumene Zone		Aplite Unit		Lepidolite Unit	
	modified host-rock		contaminated rim		magmatic core	6	7	8	9	10	11
	1	2	3	4	5						
SiO ₂ wt%	37.04	37.38	37.33	37.35	36.58	36.76	36.37	36.37	36.76	36.54	36.29
TiO ₂	0.10	0.06	0.10	0.09	0.01	0.15	0.02	0.07	0.00	0.04	0.11
Al ₂ O ₃	20.56	20.95	20.74	20.57	20.48	20.46	20.53	20.32	20.50	20.40	20.28
Fe ₂ O ₃	0.24	0.88	0.92	0.68	0.14	0.00	0.00	0.00	0.00	0.06	0.00
FeO	19.19	20.13	18.08	20.19	14.23	10.97	7.06	7.71	3.35	0.87	0.86
MnO	15.35	9.92	10.55	11.55	28.67	30.96	31.66	34.14	36.50	39.68	38.86
MgO	0.18	0.24	0.23	0.21	0.00	0.25	0.03	0.01	0.00	0.00	0.00
CaO	7.28	11.04	12.17	9.74	0.38	0.57	3.35	0.80	2.11	2.17	2.72
P ₂ O ₅	0.00	0.00	0.00	0.00	0.00	0.00	0.00	0.00	0.00	0.00	0.00
Y ₂ O ₃	0.08	0.00	0.16	0.00	0.03	0.06	0.04	0.25	0.12	0.00	0.17
ZrO ₂	0.00	0.00	0.07	0.00	0.00	0.00	0.01	0.00	0.00	0.00	0.01
Sc ₂ O ₃	0.03	0.07	0.01	0.00	0.00	0.00	0.06	0.04	0.00	0.00	0.00
F	0.00	0.00	0.00	0.00	0.00	0.00	0.00	0.00	0.00	0.03	0.23
O=F	0.00	0.00	0.00	0.00	0.00	0.00	0.00	0.00	0.00	-0.01	-0.10
Total	100.04	100.67	100.36	100.38	100.51	100.18	99.13	99.71	99.34	99.78	99.43
Si <i>apfu</i>	3.002	2.983	2.983	3.000	3.004	3.014	2.999	3.005	3.025	3.004	2.990
Ti	0.006	0.004	0.006	0.005	0.001	0.009	0.001	0.004	0.000	0.002	0.007
Al	1.964	1.970	1.953	1.947	1.982	1.977	1.995	1.978	1.988	1.976	1.969
Fe ³⁺	0.014	0.053	0.055	0.041	0.009	0.000	0.000	0.000	0.000	0.004	0.000
Fe ²⁺	1.300	1.343	1.208	1.356	0.977	0.752	0.487	0.533	0.231	0.060	0.059
Mn	1.054	0.670	0.714	0.786	1.994	2.150	2.211	2.389	2.544	2.763	2.712
Mg	0.022	0.029	0.027	0.025	0.000	0.031	0.004	0.001	0.000	0.000	0.000
Ca	0.632	0.944	1.042	0.838	0.033	0.050	0.296	0.071	0.186	0.191	0.240
P	0.000	0.000	0.000	0.000	0.000	0.000	0.000	0.000	0.000	0.000	0.000
Y	0.003	0.000	0.007	0.000	0.001	0.003	0.002	0.011	0.005	0.000	0.007
Zr	0.000	0.000	0.003	0.000	0.000	0.000	0.000	0.000	0.000	0.000	0.000
Sc	0.002	0.005	0.001	0.000	0.000	0.000	0.004	0.003	0.000	0.000	0.000
F	0.000	0.000	0.000	0.000	0.000	0.000	0.000	0.000	0.000	0.008	0.060
Total	7.999	8.001	7.999	7.998	8.001	7.986	7.999	7.995	7.979	8.008	8.044

Calculation of the formula is based on 12 anions and 8 cations. The proportion of Fe₂O₃ is inferred from charge-balance considerations.

granitic pegmatites in Ontario, garnet from the McCombe pegmatite does appear to be Ca-enriched throughout all zones (Fig. 4b). In the spodumene zone, aplite unit and lepidolite unit, the garnet attains 0.32, 0.19 and 0.24 *apfu* Ca, equivalent to 10.9, 6 and 7% of the grossular component, respectively. The McCombe dataset can best be interpreted as predominantly of pegmatite derivation, but the entire pegmatite appears to have been contaminated with Ca from host rocks. Perhaps surprisingly, given the predominance of mafic metavolcanic host-rocks in the area, garnet in the pegmatite is not similarly Mg-enriched. Possible sources for the Ca are discussed later in this paper.

TOURMALINE COMPOSITIONS

The McCombe pegmatite represents a boron-rich system in which tourmaline crystallized in all internal zones. Its greatest abundance is in the tourmalinite unit, where it forms thick foliated masses of black prismatic grains up to 5 mm in length. This schistose appearance is atypical of pegmatite crystallization; more likely, the tourmalinite unit represents remnants of leached or partially digested and recrystallized host-rocks (Fig. 5a). The tourmaline grains are strongly pleochroic and vary in color (in plane-polarized light) from straw brown to deep brown, occasionally with a bluish or orange-brown core. Compositionally, they are best described as schorl, but their relatively high Ca and Mg contents indicate that they are actually members of a schorl–uvite solid-solution series (Table 2).

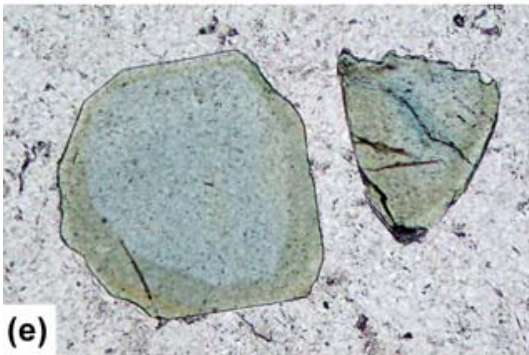
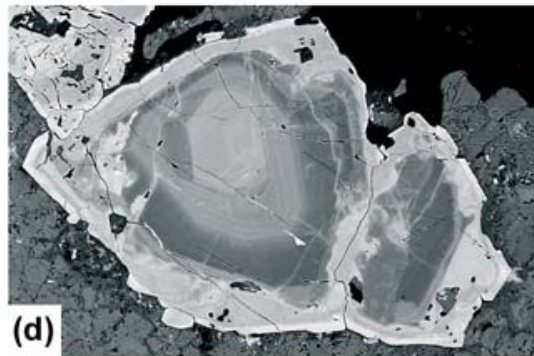
Wall-zone samples contain abundant black to deep bluish prismatic tourmaline up to 3 cm in length, with complex zonation in many samples. Progressive zonation is common and, in thin section, the colorless, pale blue or pale yellow core is rimmed with deep blue or brown tourmaline (Figs. 5b–d). The junction between core regions and the rim is complex and best described as a reaction junction. Figure 5d is a back-scattered-electron image of tourmaline from a sample of the wall zone illustrating a core region with perhaps three phases of growth (some oscillatory) and mantled with a rim that appears to be reacting (*via* thin filaments) with the core region internally and yet producing an almost euhedral external form. Collectively, the core regions of such grains define an evolutionary trend from foitite to schorl and elbaite, whereas the rim changes in composition from foitite through schorl until it reaches a composition identical to the (Ca,Mg)-rich schorl found in the tourmalinite unit.

The standard diagrams used for tourmaline classification (Figs. 6a–c) illustrate the chemical variation of tourmaline in the tourmalinite unit and the wall zone of the pegmatite. Substitution of Mg for Fe²⁺ (coupled with Ca for Na at the X site) is the reason some schorl data plot along the Y axis and outside the field of schorl in Figure 6c. It is clear from these plots that the rim of wall-zone tourmaline is intermediate in composition

between two clearly defined end-members (*i.e.*, schorl and uvite). The partially crystallized pegmatite-forming melt thus was most likely locally contaminated with mafic metavolcanic host-rocks. Crystallization of tourmaline continued, and as the host rocks were digested, they released Ca, Mg (and other elements) into the melt, causing a rapid change in composition of the later-formed tourmaline as the remaining melt solidified. It is, of course, possible that (Ca,Mg)-rich fluids migrated from the host rocks into the pegmatite-forming melt during its emplacement, but there is evidence, in the form of selvage, that makes it more likely that the contamination occurred owing to host-rock leaching or digestion (assimilation). This model of pegmatite contamination is consistent with that described by Tindle *et al.* (2002b) for petalite-subtype pegmatites elsewhere in Ontario (Fig. 6d).

In the spodumene zone, tourmaline is less common and forms black, dark blue or dark green prismatic grains that reach 1 cm in length. Tourmaline is invariably less abundant than spodumene, within which it is locally included. Under the microscope, the tourmaline usually shows a degree of progressive zonation, particularly where basal sections are encountered. Colors are pale blue or pale green (Fig. 5e). In some cases, the colored core gradually grades to an almost colorless rim (Fig. 5f). A wide range of compositions from foitite to schorl, to elbaite, and finally to “fluor-elbaite” is present in this zone (Table 2). These compositions follow the same trend as the magmatic tourmaline of the wall zone, and extend it toward more evolved compositions. A small number of rim compositions indicates that slight pegmatite – host-rock interaction has occurred in a few cases (green squares, Figs. 7a–d). Rarely, filaments with rim compositions similar to those illustrated in Figure 5d are seen infiltrating the cores of tourmaline grains, but there is no well-developed (Ca,Mg)-rich rim, as seen in tourmaline from the wall zone.

FIG. 5. Photomicrographs of tourmaline. (a) (Ca,Mg)-rich schorl (green, brown) and Ca-rich almandine (colorless) in tourmalinite unit RR10. Width of field of view 5 mm. (b) Small euhedral and larger fractured grains of foitite–schorl in wall-zone sample RR32B. Width of field of view 1.1 mm. (c, d) Crystals of foitite – schorl – (Ca,Mg)-rich schorl in wall-zone sample RR32B; photomicrograph and a back-scattered-electron (BSE) image of same grain. Width of field of view: 1.2 mm. (e) Crystals of schorl–elbaite in spodumene-zone sample RR12. Width of field of view 0.7 mm. (f) Crystal of elbaite–“fluor-elbaite” in spodumene-zone sample RR17. Width of field of view 0.85 mm. (g) Crystals of elbaite–“fluor-elbaite” in aplite-unit sample RR28. Width of field of view 2.3 mm. (h) Crystal of elbaite–“fluor-elbaite” (core) transitional to liddicoatite (rim) in lepidolite-unit sample RR11. Width of field of view 0.8 mm.



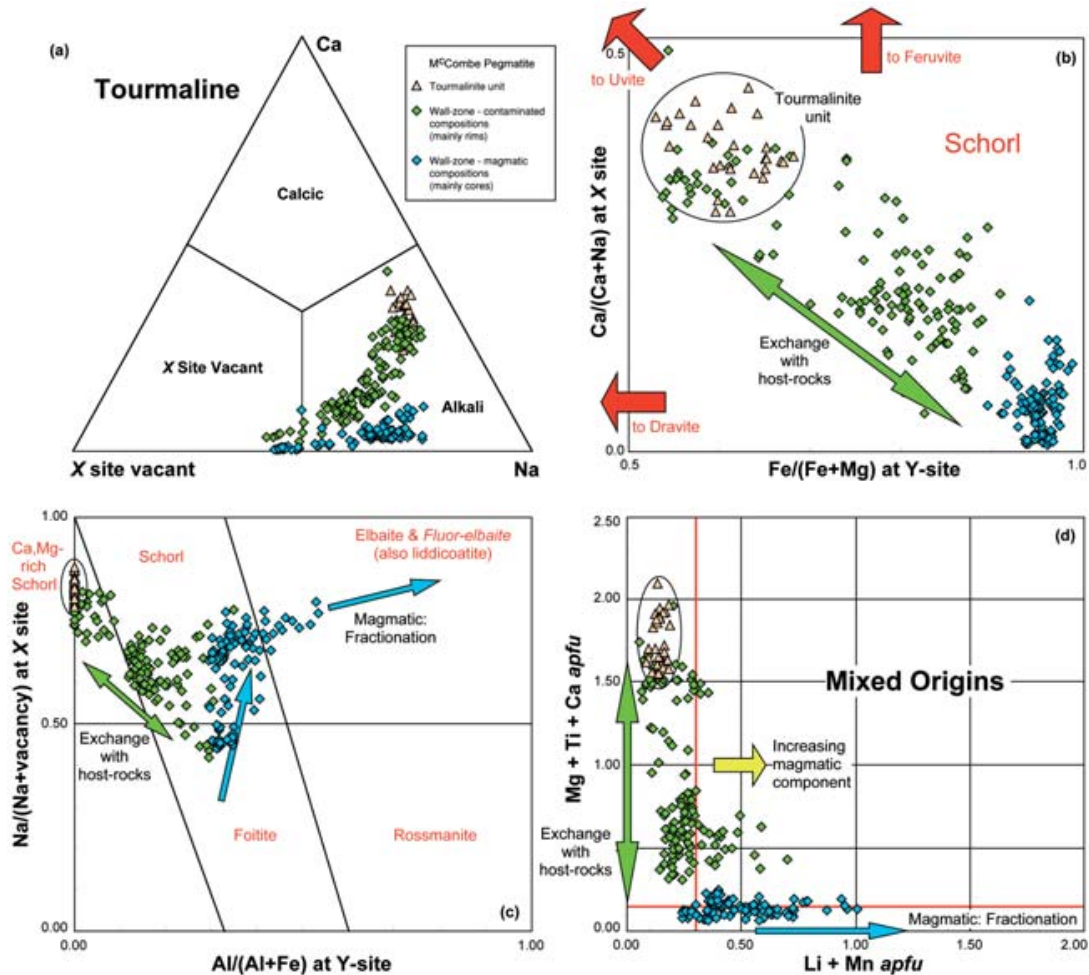


Fig. 6. Covariation in tourmaline of the schorl–uvite series from the tourmalinite unit and wall zone of the McCombe pegmatite. (a) X-site compositional variation. (b) $\text{Fe}^{2+}/(\text{Fe}^{2+} + \text{Mg})$ at the Y site versus $\text{Ca}/(\text{Ca} + \text{Na})$ at the X site. (c) $\text{Al}/(\text{Al} + \text{Fe}^{2+})$ at the Y site versus $\text{Na}/(\text{Na} + \square, \text{vacancy})$ at the X site. The limitation of plotting (Ca,Mg)-rich schorl on this diagram is shown by data from the tourmalinite unit. Despite being of schorl composition, these data plot along the Y axis and outside the field of schorl. (d) $\text{Li} + \text{Mn}$ (apfu) versus $\text{Ca} + \text{Mg} + \text{Ti}$ (apfu) after Tindle *et al.* (2002b). These diagrams illustrate the two main types of tourmaline that formed due to (i) pegmatite – host-rock interaction and (ii) an essentially magmatic process (fractional crystallization).

Spodumene-zone tourmaline initially follows a similar trend to magmatic tourmaline from the wall zone (Figs. 7a,b), starting with fottite and with increasing evolution of the pegmatite-forming melt developing schorl, elbaite and finally “fluor-elbaite” compositions. There is, however, no clear continuum of compositions on the $(\text{Li} + \text{Mn})$ versus $(\text{Mg} + \text{Ti} + \text{Ca})$ diagram (Figs. 6d, 7c), as wall-zone samples fall predominantly below the magmatic – mixed origin line ($\text{Mg} + \text{Ti} + \text{Ca} = 0.14$ apfu), whereas the spodumene-zone samples are above this line. This step in compositions suggests that mag-

matic wall-zone tourmaline crystallized from a primary uncontaminated pegmatite-forming melt and that there was a major contamination event (mainly due to an influx of Ca) before the spodumene-zone tourmaline crystallized. Some of this contamination is reflected in rim compositions of wall-zone tourmaline, but the event was sufficiently intensive that the remainder of the pegmatite-forming melt also was affected. As a result of this contamination event, tourmaline from the wall zone and the spodumene zone effectively crystallized from two similar but quite distinct parental magmas, although

their source composition was the same. The use of tourmaline compositions as a monitor of contamination has been discussed previously by Tindle et al. (2002b).

Tourmaline from the aplite unit of the pegmatite is typically dark green in color and forms smaller

(<0.5 cm), more elongate (needle-shaped) crystals than those in the spodumene zone, but both in its color under the microscope (Fig. 5g) and chemically (Fig. 7), it is similar to spodumene-zone tourmaline. Laths of tourmaline and albite in the aplite unit have a parallel orien-

TABLE 2. COMPOSITION OF TOURMALINE FROM THE MCCOMBE GRANITIC PEGMATITE, NORTHWESTERN ONTARIO

	Tourmaline Unit modified host-rock				Wall Zone contaminated				Wall Zone magmatic				Spodumene Zone			Aplite Unit		Lepidolite Unit				
	Ca,Mg Schorl		Ca,Mg Schorl		Ca,Mg Foitite		Ca,Mg Schorl		Ca,Mg Elb		Ca,Mg Foitite		Ca,Mg Elb		Ca,Mg "Fluor-Elb"		Ca,Mg Elb		Ca,Mg "Fluor-Elb"		Ca,Mg Lid	
	1	2	3	4	5	6	7	8	9	10	11	12	13	14	15	16	17	18				
SiO ₂ wt%	35.02	35.01	34.06	34.71	34.74	35.29	35.04	35.94	35.00	33.93	35.48	34.60	35.05	35.08	34.70	37.06	37.43	37.60				
TiO ₂	1.22	0.73	0.77	0.50	0.29	0.12	0.17	0.14	0.11	0.42	0.29	0.32	0.32	0.13	0.35	0.07	0.02	0.03				
Al ₂ O ₃	28.70	29.94	29.96	32.46	34.43	35.18	35.57	36.94	34.85	35.53	36.84	35.87	35.30	38.47	36.79	38.62	39.36	38.41				
FeO	11.02	11.66	12.94	13.55	12.27	11.40	9.42	6.78	10.47	8.59	5.45	8.09	8.83	1.57	6.18	1.34	0.90	0.88				
MgO	6.16	4.76	4.20	1.41	1.05	0.29	0.31	0.14	0.58	0.43	0.09	0.36	0.41	0.10	0.22	0.01	0.00	0.00				
CaO	2.13	1.41	1.70	0.78	0.24	0.05	0.29	0.46	0.06	0.39	0.96	0.35	0.34	1.50	0.61	2.14	2.44	2.75				
MnO	0.08	0.06	0.08	0.24	0.34	0.81	0.89	1.58	0.80	0.94	1.70	1.06	0.97	3.79	1.29	2.05	1.77	1.43				
ZnO	0.04	0.09	0.13	0.45	0.52	1.79	2.16	0.56	1.93	2.33	1.77	2.44	1.95	0.47	2.49	0.36	0.36	0.44				
Na ₂ O	1.62	1.80	1.65	1.65	1.30	1.41	2.01	2.14	1.51	1.92	2.02	2.12	2.04	1.92	2.15	1.51	1.35	1.16				
K ₂ O	0.03	0.03	0.02	0.03	0.03	0.02	0.03	0.01	0.02	0.03	0.02	0.02	0.03	0.02	0.00	0.01	0.01	0.01				
F	0.41	0.40	0.35	0.15	0.00	0.14	0.44	0.84	0.37	0.44	0.87	0.57	0.63	1.18	0.93	1.18	1.15	1.26				
Cl	0.00	0.00	0.01	0.01	0.01	0.00	0.01	0.00	0.00	0.00	0.00	0.00	0.01	0.00	0.00	0.01	0.01	0.00				
H ₂ O*	3.36	3.35	3.33	3.47	3.55	3.53	3.40	3.27	3.48	3.45	3.25	3.08	3.36	3.11	3.19	3.19	3.25	3.17				
B ₂ O ₃ *	10.31	10.27	10.16	10.26	10.30	10.42	10.46	10.63	10.34	10.61	10.60	10.64	10.64	10.64	10.51	10.89	11.02	10.93				
Li ₂ O*	0.18	0.20	0.11	0.31	0.22	0.28	0.62	1.14	0.28	0.61	1.23	1.58	0.73	1.57	0.98	2.04	2.17	2.28				
Total	100.29	99.72	99.48	99.98	99.31	100.72	100.81	100.57	99.79	99.62	100.55	101.12	100.63	99.55	100.40	100.48	101.23	100.35				
O=F	0.17	0.17	0.15	0.06	0.00	0.06	0.18	0.35	0.15	0.19	0.37	0.24	0.27	0.50	0.39	0.50	0.48	0.53				
Total*	100.11	99.55	99.33	99.92	99.31	100.66	100.63	100.21	99.63	99.44	100.18	100.87	100.36	99.06	100.01	99.98	100.74	99.82				
T Si <i>apfu</i>	5.903	5.928	5.829	5.879	5.859	5.885	5.823	5.874	5.903	5.727	5.818	5.859	5.840	5.729	5.740	5.916	5.906	5.979				
Al	0.097	0.072	0.171	0.121	0.141	0.115	0.177	0.126	0.097	0.273	0.182	0.141	0.160	0.271	0.260	0.084	0.094	0.021				
B	3.000	3.000	3.000	3.000	3.000	3.000	3.000	3.000	3.000	3.000	3.000	3.000	3.000	3.000	3.000	3.000	3.000	3.000				
Z Al	5.605	5.902	5.873	6.000	6.000	6.000	6.000	6.000	6.000	6.000	6.000	6.000	6.000	6.000	6.000	6.000	6.000	6.000				
Mg	0.395	0.098	0.127	0.000	0.000	0.000	0.000	0.000	0.000	0.000	0.000	0.000	0.000	0.000	0.000	0.000	0.000	0.000				
Fe ³⁺	0.000	0.000	0.000	0.000	0.000	0.000	0.000	0.000	0.000	0.000	0.000	0.000	0.000	0.000	0.000	0.000	0.000	0.000				
Y Al	0.000	0.000	0.000	0.360	0.703	0.800	0.790	0.991	0.796	0.796	0.937	1.084	0.772	1.134	0.913	1.180	1.225	1.176				
Ti	0.154	0.093	0.099	0.064	0.037	0.015	0.021	0.017	0.014	0.053	0.035	0.016	0.041	0.016	0.044	0.008	0.003	0.003				
Fe ³⁺	0.000	0.000	0.000	0.000	0.000	0.000	0.000	0.000	0.000	0.000	0.000	0.000	0.000	0.000	0.000	0.000	0.000	0.000				
Mg	1.152	1.103	0.945	0.357	0.264	0.073	0.076	0.035	0.143	0.109	0.021	0.013	0.101	0.025	0.054	0.001	0.000	0.001				
Mn	0.011	0.008	0.012	0.035	0.048	0.114	0.125	0.219	0.122	0.135	0.236	0.417	0.136	0.524	0.180	0.278	0.236	0.192				
Fe ²⁺	1.554	1.651	1.852	1.920	1.731	1.589	1.309	0.927	1.513	1.212	0.748	0.386	1.231	0.214	0.855	0.179	0.118	0.117				
Zn	0.005	0.011	0.016	0.056	0.065	0.221	0.265	0.067	0.222	0.291	0.214	0.044	0.240	0.057	0.304	0.042	0.042	0.051				
Li*	0.124	0.135	0.076	0.214	0.151	0.188	0.414	0.747	0.190	0.405	0.808	1.041	0.479	1.030	0.649	1.312	1.377	1.460				
Sum	3.000	3.002	3.000	3.005	2.999	2.999	3.000	3.001	3.000	3.000	3.000	3.000	3.000	3.000	3.000	3.000	3.000	3.000				
X Ca	0.385	0.256	0.312	0.142	0.043	0.009	0.052	0.081	0.009	0.070	0.169	0.210	0.060	0.262	0.108	0.366	0.413	0.469				
Na	0.531	0.592	0.546	0.543	0.426	0.455	0.648	0.677	0.441	0.629	0.642	0.642	0.658	0.607	0.688	0.468	0.413	0.357				
K	0.006	0.006	0.004	0.006	0.006	0.004	0.007	0.003	0.005	0.006	0.003	0.004	0.007	0.005	0.005	0.000	0.002	0.003				
□	0.078	0.146	0.138	0.309	0.524	0.532	0.294	0.239	0.545	0.294	0.186	0.144	0.274	0.127	0.199	0.166	0.173	0.171				
OH	3.779	3.787	3.805	3.919	3.997	3.928	3.769	3.564	3.898	3.763	3.550	3.357	3.665	3.390	3.515	3.401	3.425	3.367				
F	0.220	0.213	0.191	0.079	0.000	0.072	0.230	0.436	0.102	0.236	0.450	0.643	0.333	0.610	0.485	0.597	0.574	0.633				
Cl	0.001	0.000	0.004	0.002	0.003	0.000	0.001	0.000	0.000	0.001	0.000	0.000	0.003	0.000	0.000	0.002	0.001	0.000				

Structural formulae are based on 31 anions (O, OH, F). * The proportions of H₂O, B₂O₃ and Li₂O are calculated on the basis of stoichiometry. Mineral symbols used: Elb: elbaite, "Fluor-elb": "fluor-elbaite", Lid: liddicoatite. Ca,Mg schorl is an abbreviated way of saying (Ca,Mg)-enriched schorl.

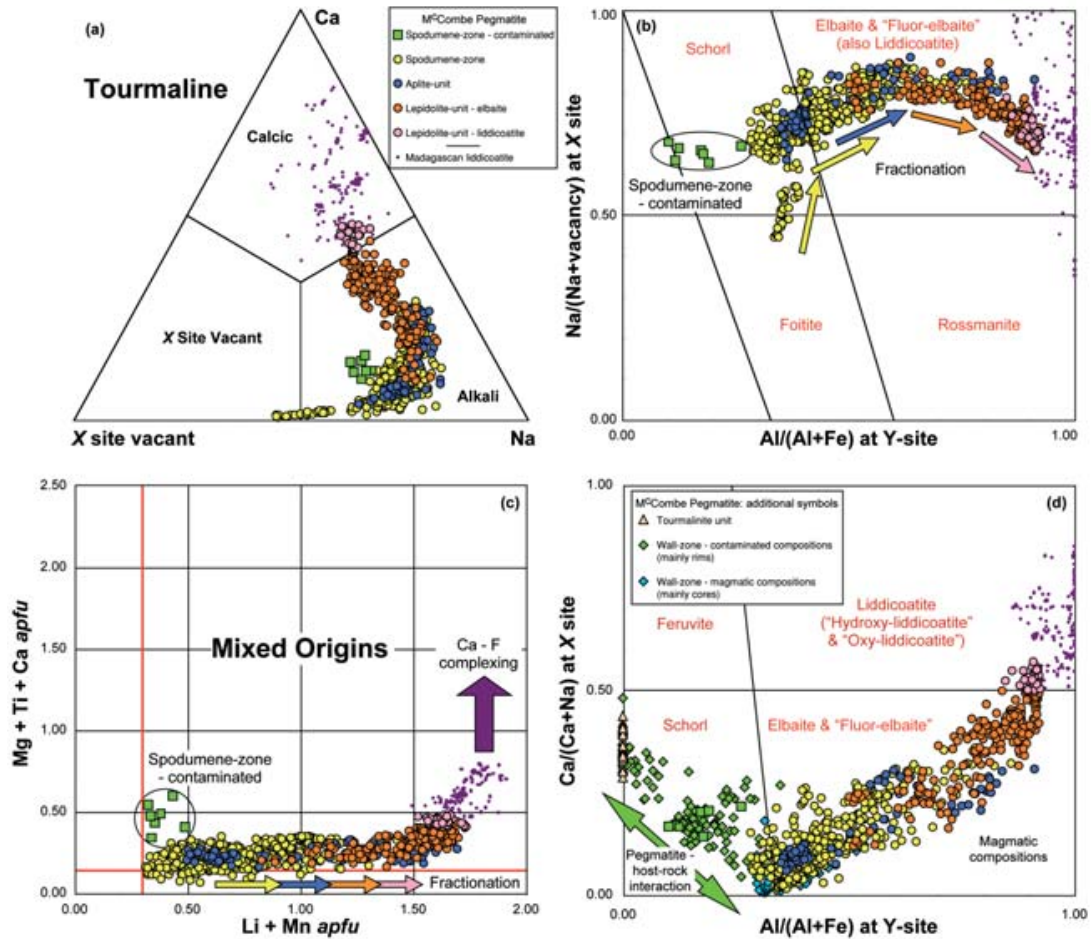


Fig. 7. Covariation in tourmaline of the foitite – schorl – elbaite – “fluor-elbaite” series from the spodumene zone and aplite unit of the McCombe pegmatite. Data on elbaite – “fluor-elbaite” – liddicoatite from the lepidolite unit also are plotted and compared with selected data on liddicoatite from Madagascar (Dirlam *et al.* 2002; A.G. Tindle, unpubl. data). (a) Compositional variation at the X site. (b) Al/(Al + Fe) at the Y site versus Na/(Na + □, vacancy) at the X site. See Selway *et al.* (1999) for further explanation of boundaries between species. (c) Li + Mn (apfu) versus Ca + Mg + Ti (apfu) after Tindle *et al.* (2002b). See Selway (d) Al/(Al + Fe²⁺) at the Y site versus Ca/(Ca + Na) at the X site. Note that this diagram does not account for Li in elbaite and liddicoatite.

tation that gives the samples a foliated texture. Spodumene is less common in the aplite unit than in the spodumene zone.

There is a great deal of overlap in the compositional range of spodumene-zone and aplite-unit tourmaline (Figs. 7a,b), although foitite is absent from the latter. This overlap is consistent with the hypothesis that the aplite unit formed slightly later than the spodumene zone. In the Bob Ingersoll pegmatite, Black Hills, South Dakota, the overlap suggests a high degree of interzonal communication during crystallization. Alternatively, such overlaps in composition may result from extreme

fractionation during late crystallization of one zone, overlapping with early crystallization of a later zone (Jolliff *et al.* 1987). There does not appear to have been additional contamination of the pegmatite-forming melt between the spodumene zone and the aplite unit of the McCombe pegmatite, as there is no step in (Mg + Ca + Ti) content between them (Fig. 7c).

The lepidolite unit of the McCombe pegmatite is spatially quite small, occurring as mica-rich pods and seams particularly close to the southern margin of Dyke 1. It is, however, an important component of the pegmatite, as it crystallized from the most evolved part of

the pegmatite-forming melt (or perhaps from residual fluids) and is the host for liddicoatite. In this unit, tourmaline is a rare phase, forming tiny (<0.25 mm) olive-green needle-shaped crystals among the foliated albite and lepidolite. Figures 7b and 7c show that the tourmaline from this unit is overall more evolved than that from earlier zones, with a compositional range from elbaite to “fluor-elbaite” and to liddicoatite. Even in an individual crystal, these three species can be found, with elbaite forming the core, and liddicoatite, the rim. These different species are not distinguishable in an optical image (Fig. 5h).

Figure 7d shows the entire dataset for tourmaline from the McCombe pegmatite. With it, we define a new diagram for the classification of (Li–Ca)-dominant tourmaline. This diagram has the advantage of being able to display both tourmaline that has undergone pegmatite – host-rock interaction [foitite – schorl – (Ca,Mg)-rich schorl] and magmatic tourmaline (foitite – schorl – elbaite – “fluor-elbaite” – liddicoatite) as linear arrays, and it also allows elbaite and liddicoatite to be distinguished. It does not pick out the step in composition from wall-zone to spodumene-zone tourmaline, nor does it display (Ca,Mg)-rich tourmaline well (these data fall along the Y axis). Thus it does have limitations and should be used in conjunction with other diagrams. Boundaries between species have been calculated by initially establishing the end-member values: elbaite: $Al/(Al + Fe) = 1.5/1.5 = 1$, $Ca/(Ca + Na) = 0$; schorl: $Al/(Al + Fe) = 0$, $Ca/(Ca + Na) = 0$; liddicoatite: $Al/(Al + Fe) = 1/1 = 1$, $Ca/(Ca + Na) = 1/1 = 1$; feruvite: $Al/(Al + Fe) = 0$, $Ca/(Ca + Na) = 1/1 = 1$. For clarity, the end-member compositions are not plotted on Figure 7d. The mid-point between schorl and elbaite at the Y site contains $Fe_{1.5}Al_{0.75}Li_{0.75}$, and corresponds to $Al/(Al + Fe) = 0.75/(0.75 + 1.5) = 0.3333$, $Ca/(Ca + Na) = 0$. The mid-point between feruvite and liddicoatite at the Y site contains $Fe_{1.5}Al_{0.5}Li_{1.0}$, and corresponds to $Al/(Al + Fe) = 0.5/(0.5 + 1.5) = 0.25$, $Ca/(Ca + Na) = 1$.

LITHIUM VARIATION IN TOURMALINE

Lithium has already been shown to vary markedly during the evolution of tourmaline compositions in petalite-subtype (Selway *et al.* 2000, 2002, Tindle *et al.* 2002b), lepidolite-subtype (Selway *et al.* 1999) and elbaite-subtype pegmatites (Selway *et al.* 1999, Novák & Povondra 1995). It is our purpose in this section to discuss the behavior of lithium in the McCombe pegmatite, a spodumene-subtype pegmatite (albeit an unusual one). To aid comparisons, the format of the diagrams follows that of Tindle *et al.* (2002b), who summarized why Li has been chosen as an indicator of fractionation. These diagrams are particularly useful for examining substitution schemes too, as many tourmaline end-member compositions can be represented on them.

Li versus Mg covariation

Magnesium (at the Y site) is uniformly low in all magmatic samples from the McCombe pegmatite, varying from ≤ 0.2 apfu to 0.1 apfu as Li approaches 0.8 apfu (Fig. 8a). At this point, there is a small step to lower Mg nearer 0.05 apfu, before further fractionation (shown by increasing Li values) takes compositions to near the Mg detection limit in the liddicoatite samples. The step coincides with the end of wall-zone crystallization, but crystallization of the spodumene zone, aplite unit and lepidolite unit crosses over it. Compositions of tourmaline from the tourmalinite unit, rim compositions of wall-zone tourmaline and a few compositions of contaminated spodumene-zone tourmaline define a low-Li – high-Mg array consistent with the crystallization of rim compositions after the pegmatite-forming melt interacted with Mg-rich host-rocks. A similar pattern of variation (but with more scatter) occurs with Ti (not depicted here). Not apparent from Figure 8a is the significant Mg at the Z site ($Mg \leq 0.4$ apfu) in the tourmalinite unit and in some rims from the wall zone (Table 2).

Li versus Fe^{2+} covariation

Figure 8b illustrates the major Y-site substitution scheme operating in magmatic tourmaline in the McCombe pegmatite: $2Fe^{2+} \Leftrightarrow Al + Li$. In the tourmalinite and contaminated wall-zone samples, this substitution still operates, but is replaced by $Fe^{2+} \Leftrightarrow (Mg + Ti)$ substitution in certain Mg-rich samples. As a peculiarity of this diagram, it shows a linear trend from foitite to elbaite and excludes schorl compositions, but this anomaly arises because other Y-site data are not plotted.

Li versus Al covariation

Aluminum is plotted separately from Fe^{2+} to illustrate a further scheme of substitution operating on the most evolved lepidolite-unit samples (Fig. 8c). Unlike many of the liddicoatite compositions from Madagascar (Dirlam *et al.* 2002), which fall along an elbaite-liddicoatite line, the liddicoatite data from the McCombe pegmatite fall along a line that more closely follows an “oxy-manganofoitite” to liddicoatite substitution. The remaining magmatic samples form a linear array dominated by the $2Fe^{2+} \Leftrightarrow Al + Li$ substitution. All the contaminated wall-zone samples drop off this array to lower Al values, where they become Al-deficient (at the Y site) in the (Ca,Mg)-rich schorl of the tourmalinite unit.

Li versus Mn covariation

The pattern of manganese variation in magmatic tourmaline from the McCombe pegmatite is very different from that of other elements discussed so far, as

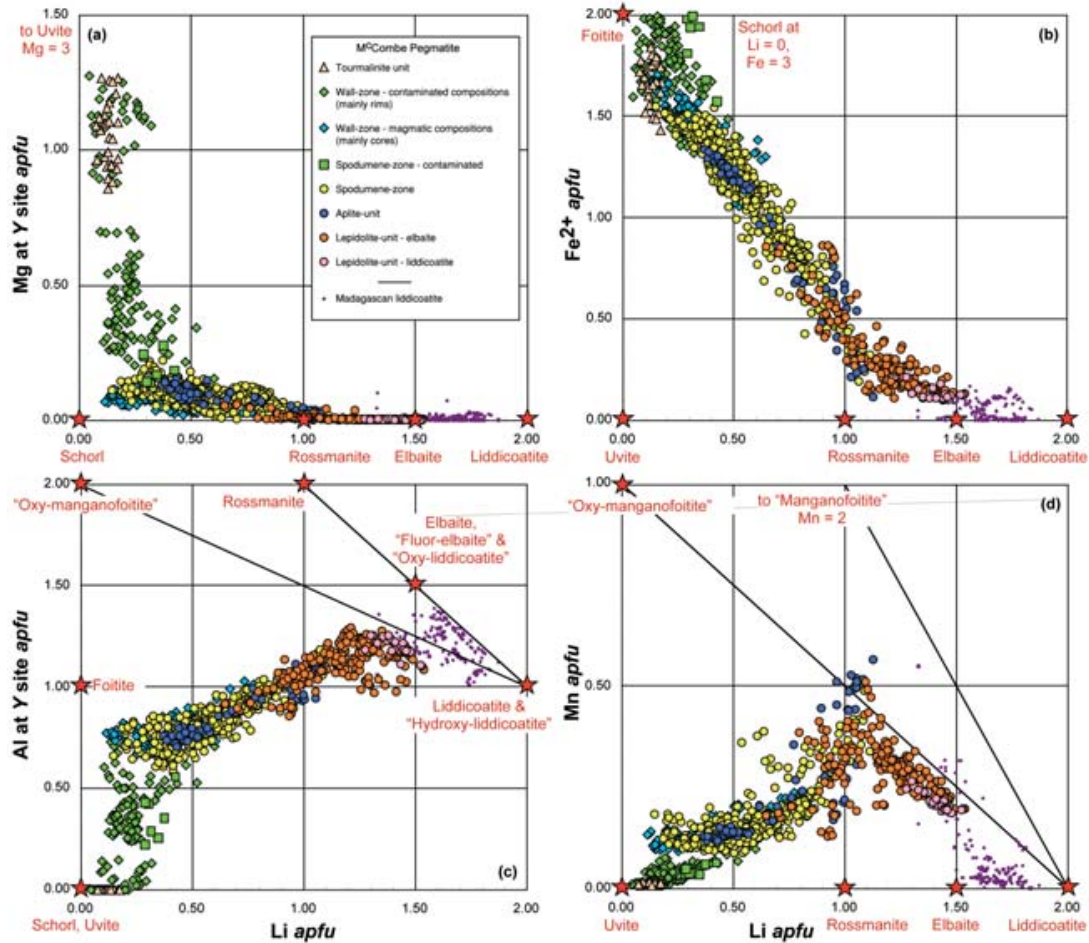


Fig. 8. Covariation of Li with other Y-site cations in tourmaline from the McCombe pegmatite, compared with selected data on liddicoatite from Madagascar (Dirlam *et al.* 2002; A.G. Tindle, unpubl. data). (a) Li versus Mg (apfu). (b) Li versus Fe²⁺ (apfu). (c) Li versus Al (apfu). (d) Li versus Mn (apfu).

with increasing Li, there is first a rise (to above 0.5 apfu Mn) followed by a steep drop to 0.2 apfu Mn in the most evolved liddicoatite-bearing sample (Fig. 8d). A similar pattern was observed in tourmaline from the Black Hills, South Dakota by Jolliff *et al.* (1986). They explained this trend as one of a sequence of hiatuses caused by high-field-strength elements being favored at higher temperatures, and the successively lower field-strength elements, ideally peaking at lower temperatures. Using Fe + Mg as an index of increasing fractionation and decreasing temperature index, Jolliff *et al.* (1986) predicted maximum Y-site occupancies in the order Ti, Mg, Fe, Zn, Mn, (Li + Al) and were able to show how important a factor crystal-chemical control is on the overall compositional trends of tourmaline.

In Figure 8d, we show the development of the “oxy-manganofoitite” to liddicoatite substitution in the lepidolite unit. This substitution scheme ($\square + \text{Mn} + \text{Al} \Leftrightarrow \text{Ca} + \text{Li}_2$) has apparently not been described previously, although Tindle *et al.* (2002b) have described the mechanism of the “oxy-manganofoitite” to elbaite substitution in tourmaline from the Separation and Pakeagama Lake pegmatites of northwestern Ontario. What is not obvious from Figure 8d is why there is such a wide scatter in data on magmatic tourmaline at Li = 1.0 apfu. It may be that at this point in the crystallization sequence, the crystallization of lepidolite-group minerals began, into which Mn was preferentially partitioned.

Li versus Zn covariation

The observed negative correlation of Zn with Li in magmatic tourmaline from the McCombe pegmatite is very different from the prediction of a Zn hiatus at a higher temperature than Mn, as discussed by Jolliff *et al.* (1986). There also appears to be three subparallel Zn trends, offset to slightly higher Li values in the order wall zone, spodumene zone and aplite unit (combined), and lepidolite unit. This trend can be explained by the formation of individual zones with a certain degree of independence from one another. It is possible that Zn concentrations in wall-zone tourmaline may have been lowered owing to contamination effects; metasomatized holmquistite-bearing host-rocks close to the pegmatite have much higher Zn contents (95–215 ppm) than unaltered host-rocks further away (51–74 ppm), however, indicating that Zn is moving out of the pegmatite, rather than moving into it from the host rocks.

Although Zn is normally considered a trace element in tourmaline, its concentration reaches 2.5 wt.% ZnO (equivalent to 0.3 *apfu*) in schorl from the McCombe pegmatite, an abundance not reported in tourmaline from other LCT pegmatites.

Li versus Na covariation

Apart from a small offset in the data from the tourmalinite unit and some rim compositions from contaminated wall-zone samples, tourmaline from the McCombe pegmatite defines a curvilinear trend that starts at 0.4 *apfu* Na (foitite), increases through schorl to elbaite compositions with a hiatus at 0.6 *apfu* Li, 0.8 *apfu* Na and then drops to 1.5 *apfu* Li, 0.35 *apfu* Na as liddicoatite crystallized (Fig. 9b). The pattern is essentially one of gradual change in X-site occupancy from dominantly X-site vacant to first Na- and then Ca-dominant tourmaline.

The initial trend of increasing Na with evolution of the pegmatite-forming melt is also paralleled by fluorine. Robert *et al.* (1997) were able to show that this trend of increasing Na at the X site with F at the W site is due to crystal-chemical constraints and to $f(F_2)$. The spodumene-subtype McCombe pegmatite is yet another example of this behavior and complements other complex-type pegmatites, including lepidolite-subtype pegmatites from the Czech Republic (Selway *et al.* 1999, Novák 2000) and petalite-bearing pegmatites from northwestern Ontario (Tindle *et al.* 2002b), Manitoba (Selway *et al.* 2000) and Sweden (Selway *et al.* 2002).

After the hiatus in Na, the McCombe pegmatite continues to evolve by crystallizing tourmaline with increasingly higher Ca contents, and eventually this leads to liddicoatite formation. Many other LCT pegmatites do not do this; instead, the melt crystallizes X-site-vacant tourmaline that either approaches or crystallizes as rossmanite. The reduction of Na in tourmaline also

correlates with an increase in the abundance of albite, such that some rocks are essentially albitites. A drop in Na content of tourmaline is definitely not caused by depletion of this element in evolved pegmatite-forming melt, but rather a change in the partitioning between tourmaline and albite.

Li versus Ca covariation

Unlike the Na trend observed in tourmaline data from magmatic samples of the McCombe pegmatite, Ca defines a much more linear trend, ranging from near the detection limit in the core of wall-zone tourmaline to 0.46 *apfu* in the most evolved liddicoatite-bearing sample (Fig. 9c). This increasing availability of Ca for tourmaline crystallization during fractionation of the pegmatite is what makes the McCombe pegmatite so unusual. It is not unique, however, as tourmaline from the liddicoatite-bearing pegmatites in Madagascar apparently follow the same pattern (Fig. 9c), as does the Blizná pegmatite in the Czech Republic (Novák *et al.* 1999), the High Grade Dyke, Manitoba (Teertstra *et al.* 1999a) and, to a lesser extent, the Bob Ingersoll pegmatite, Black Hills, South Dakota (Jolliff *et al.* 1986) and Marko's pegmatite, one of the Separation Rapid pegmatites in Ontario (Tindle *et al.* 2002b). Laurs *et al.* (1998) also reported Ca enrichment in late-crystallized tourmaline from miarolitic granitic pegmatites from the Nanga Parbat region of northern Pakistan.

Li versus F covariation

Figure 9d illustrates a strong positive correlation of Li with F in tourmaline data from magmatic samples of the McCombe pegmatite and indicates increased F activity as fractionation progressed in the pegmatite. Evolved compositions from the spodumene-zone and aplite-unit samples have sufficient F that they cross the boundary from elbaite to "fluor-elbaite" at $F > 0.5$ *apfu*, and in the lepidolite unit, most of the tourmaline is F-dominant. This increased activity of F also contributed to an identical pattern of Li and F enrichment in lepidolite from the McCombe pegmatite (A.G. Tindle, unpubl. data), a correlation not found in lepidolite-subtype pegmatites (Selway *et al.* 1999).

The increase in F and Ca in tourmaline throughout the evolution of the McCombe pegmatite (Figs. 9c,d) is compatible with Ca-F complexing and may explain the late crystallization of microlite instead of manganotantalite, and incorporation of F into garnet from the lepidolite unit, as both Ca and F were able to be conserved until the last stages of pegmatite crystallization. A further observation from Figure 9d and, to lesser extents, the Na (Fig. 9b) and Ca (Fig. 9c) diagrams, is how far away the Ca- and Mg-rich schorl compositions from the tourmalinite unit appear to be, not only from the uvite end-member, but also from end-member schorl.

As none of the tourmaline classification diagrams or Li plots can adequately describe all the species variations, they are summarized in Table 3.

Comparison with liddicoatite from Madagascar

Liddicoatite from the McCombe pegmatite has a restricted composition if compared to that from Madagascar. This finding is best illustrated in Figure 7a, where the McCombe data plot close to the boundary between alkali and calcic tourmalines, whereas the Madagascar data fill much of the calcic tourmaline field and trend toward end-member liddicoatite (Figs. 8, 9). Some of the scatter in the Madagascar data reflects the fact that they are compiled from different localities and sources (Dirlam *et al.* 2002), but the overall trend is that of an extension beyond compositions found at McCombe and consistent with what appears to be crystallization from a more evolved (Ca,Li)-rich, Fe-poor source. For clarity, what has not been shown on these diagrams is the remainder of the Madagascar dataset, which are of elbaite and "fluor-elbaite" compositions (they would have overlapped most of the McCombe data). On the basis of these data, the processes controlling tourmaline substitution at both locations are most likely the same, with the Madagascar data reflecting an extreme development.

DISCUSSION

So where did the Ca come from, and how was it able to be retained in the pegmatite-forming melt to such a late stage in the fractionation sequence that liddicoatite was able to form? Or was it really in the melt?

Mafic metavolcanic rocks (now amphibolitized) surrounding the McCombe pegmatite contain calcite away from the general area of the pegmatite, but near the pegmatite contact and in selvage material, calcite is absent, so it clearly could have been incorporated into the melt. Also as the contact with the pegmatite is approached, there is a replacement within the amphibolite of hornblende (magnesian hornblende) by holmquistite, and a consequent exchange of $\text{Ca} + (\text{Mg}, \text{Fe}^{2+}) \Rightarrow \text{Li}_2 + \text{Si}$ resulted. Some of this Ca formed epidote, but perhaps not all. In selvage material, in particular, the Ca could have been incorporated into the melt during the assimilation-leaching process. Calc-silicate segregations generally comprised of calcite, calcic plagioclase, epidote, quartz and garnet, are ubiquitous in pillowed mafic metavolcanic rocks of the Superior Province (based upon the authors' field observations) and have been noted around the McCombe pegmatite. Such segregations thus constitute another potential source of Ca.

In their discussion of boron metasomatism around the Tanco pegmatite of Manitoba, Morgan & London (1987) were able to show that the amphibolite, with an initial assemblage of hornblende + plagioclase \pm biotite

\pm apatite, was replaced by tourmaline + quartz \pm epidote \pm zoisite \pm titanite \pm apatite \pm holmquistite \pm chlorite \pm clays \pm calcite. It is easy to see that if this process acted on selvage caught up in pegmatite-forming melt, Ca from calcite could readily be incorporated into that melt. Liddicoatite is not found at Tanco, so if this was a process capable of enriching pegmatite-forming melt in Ca, then the implication is that the McCombe pegmatite assimilated more host-rock than Tanco pegmatite or (less likely) that the physicochemical properties of the melts were different.

Another source of Ca may have been the clastic metasedimentary rocks, such as a poorly exposed metawacke unit outcropping within 50 meters on either side of the liddicoatite locality. The metawacke is not particularly Ca-rich, although it does contain calcic plagioclase, with minor hornblende, apatite, epidote and titanite. The most attractive solution to explain the high Ca contents of tourmaline from the McCombe pegmatite would be the assimilation of calcareous metasedimentary rocks such as dolomitic limestone or marble. Such rocks are rare in the Superior Province of Ontario, however (Hoffman 1985).

The process most likely delaying the onset of Ca precipitation until late in pegmatite evolution is that of Ca-F complexing. Sequestering of some Ca in melt as fluoride complexes was suggested by Weidner & Martin (1987) for leucogranite containing primary fluorite. Since then, Laurs *et al.* (1998) have suggested that this process was involved in the evolution of silicate-rich aqueous fluids as they crystallized to form miarolitic pegmatites in northern Pakistan, and more recently, Selway *et al.* (2000), Tindle *et al.* (2002b), and Selway *et al.* (2002) have suggested that the process was active during the late-stage development of petalite-subgroup pegmatites in Manitoba, northwestern Ontario, and Sweden, respectively. Garnet with a calcic rim (up to 0.24 apfu Ca) and high F content (up to 0.23 wt.% F) in the lepidolite unit of the McCombe pegmatite could also have developed in this way.

There is also a possibility that Ca could have been introduced at a low temperature, possibly in a hydrothermal stage of evolution of the pegmatite. We consider this unlikely, as such an event would also make Mg available to crystallizing tourmaline, as the host rocks are both Ca- and Mg-rich. Liddicoatite is only one of the species with elevated Ca contents (garnet, microlite and fluorapatite are others), and it would be difficult to crystallize these hydrothermally. In addition, liddicoatite forms euhedral crystals, as might be expected in a magmatic environment, and does not occur in late-stage fractures or in any form of miarolitic cavity more normally associated with the hydrothermal stage of crystallization.

Although a detailed petrogenetic model for the origin of the Madagascar pegmatites has not been established, there can be little doubt that contamination of

the pegmatite-forming melt by marble and dolomitic carbonate was of major importance (Dirlam *et al.* 2002). This is in contrast to the conclusion arrived at by Novák *et al.* (1999), who interpreted the liddicoatite-bearing, elbaite-subtype Blizná pegmatite in the Czech Republic as having crystallized from an uncontaminated (Na, Al, Li, B)-rich pegmatite-forming melt. This latter conclusion is supported by Teertstra *et al.* (1999a), who argued that the liddicoatite-bearing spodumene-subtype High Grade Dyke of Manitoba did not experience an influx of Ca from the host rocks and instead fractionated liddicoatite from an uncontaminated melt of unusual bulk-composition.

All the evidence suggests that the McCombe pegmatite was contaminated by the host rocks and that through a process of leaching and assimilation, Ca, Mg and Ti were introduced into the pegmatite-forming melt. In summary (Fig. 10), the following sequence of events is considered to have occurred:

1. Intrusion of uncontaminated, pegmatite-forming melt into amphibolitized mafic metavolcanic and metasedimentary host-rocks (wall-zone tourmaline crystallizes with a core of foitite composition). Selvedges of host rocks entrained in the pegmatites are tourmalinized.

2. Pegmatite-forming melt reacts with entrained host-rocks and a mingled composition results, with rim compositions of wall-zone tourmaline crystallizing in a disequilibrium environment. Tourmaline compositions formed at this time are intermediate in composition between those found in the tourmalinite unit and the cores of wall-zone tourmaline. These tourmaline grains have high Mg and Ti contents. As the temperature dropped, Mg and Ti were not held by the pegmatite-forming melt in any significant amount; they are preferentially retained by the residual tourmalinite unit.

3. Leaching and assimilation of the host rocks and selvedge continue, with Mg, Ti and Ca all being incorporated into what is now a well-mixed, contaminated pegmatite-forming melt. The spodumene zone begins to form from this melt, and foitite crystallizes. Calcium from the exchange with host rocks is preferentially held by the pegmatite-forming melt.

4. The formation of the wall zone and that of the spodumene zone progress almost independently, as if from two separate melts. The difference is apparent on Figures 6d, 7c and 10. It is possible that the wall zone formed before much of the spodumene zone had crystallized. There is a progressive change in tourmaline compositions from foitite, to schorl, and then to elbaite.

TABLE 3. SUMMARY OF TOURMALINE SPECIES AND SUBSTITUTIONS DESCRIBED IN THE TEXT

Species	Formulae				Tur unit (m.h.r.)	Wall zone (c.r.)	Wall zone (m.c.)	Spd zone (c.r.)	Spd zone	Aplite unit	Lpd unit
	X site	Y site	Z site	W site							
Uvite	Ca	Mg ₃	MgAl ₅	Si ₆ O ₁₈ (BO ₃) ₃ (OH) ₃	F	(x)	(x)				
Schorl	Na	(Fe ²⁺) ₃	Al ₆	Si ₆ O ₁₈ (BO ₃) ₃ (OH) ₃	(OH)		x	x			
Foitite	□	(Fe ²⁺) ₂ Al	Al ₆	Si ₆ O ₁₈ (BO ₃) ₃ (OH) ₃	(OH)		x	x	x		
Elbaite	Na	Li _{1.5} Al _{1.5}	Al ₆	Si ₆ O ₁₈ (BO ₃) ₃ (OH) ₃	(OH)		x	x	x	x	
“Fluor-elbaite”	Na	Li _{1.5} Al _{1.5}	Al ₆	Si ₆ O ₁₈ (BO ₃) ₃ (OH) ₃	F			x	x	x	x
Liddicoatite	Ca	Li ₂ Al	Al ₆	Si ₆ O ₁₈ (BO ₃) ₃ (OH) ₃	F						x
“Oxy-liddicoatite”	Ca	Li _{1.5} Al _{1.5}	Al ₆	Si ₆ O ₁₈ (BO ₃) ₃ (OH) ₃	O						
“Hydroxy-liddicoatite”	Ca	Li ₂ Al	Al ₆	Si ₆ O ₁₈ (BO ₃) ₃ (OH) ₃	(OH)						
“Oxy-manganofoitite”	□	MnAl ₂	Al ₆	Si ₆ O ₁₈ (BO ₃) ₃ (OH) ₃	O						
“Manganofoitite”	□	Mn ₂ Al	Al ₆	Si ₆ O ₁₈ (BO ₃) ₃ (OH) ₃	(OH)						
Rossmannite	□	LiAl ₂	Al ₆	Si ₆ O ₁₈ (BO ₃) ₃ (OH) ₃	(OH)						

Substitution schemes											
uvite – schorl						x	x				
foitite – schorl								x			
schorl – elbaite								x		x	
elbaite – “fluor-elbaite”									x	x	
“fluor-elbaite” – liddicoatite											x
“oxy-manganofoitite” – liddicoatite											x

Species names in quotes are not formally recognized by the IMA. For each unit or zone, x indicates the occurrence of a species or substitution scheme. (x): uvite is not found in the McCombe pegmatite, but the (Ca,Mg)-rich schorl in the tourmalinite unit and wall-zone approaches the uvite field in composition (see Fig. 6b). Tur unit: tourmalinite unit (m.h.r.: modified host-rocks). Wall zone (c.r.: contaminated rims). Wall zone (m.c.: magmatic cores). Spodumene zone (c.r.: contaminated rims). Spd: spodumene, Lpd: lepidolite.

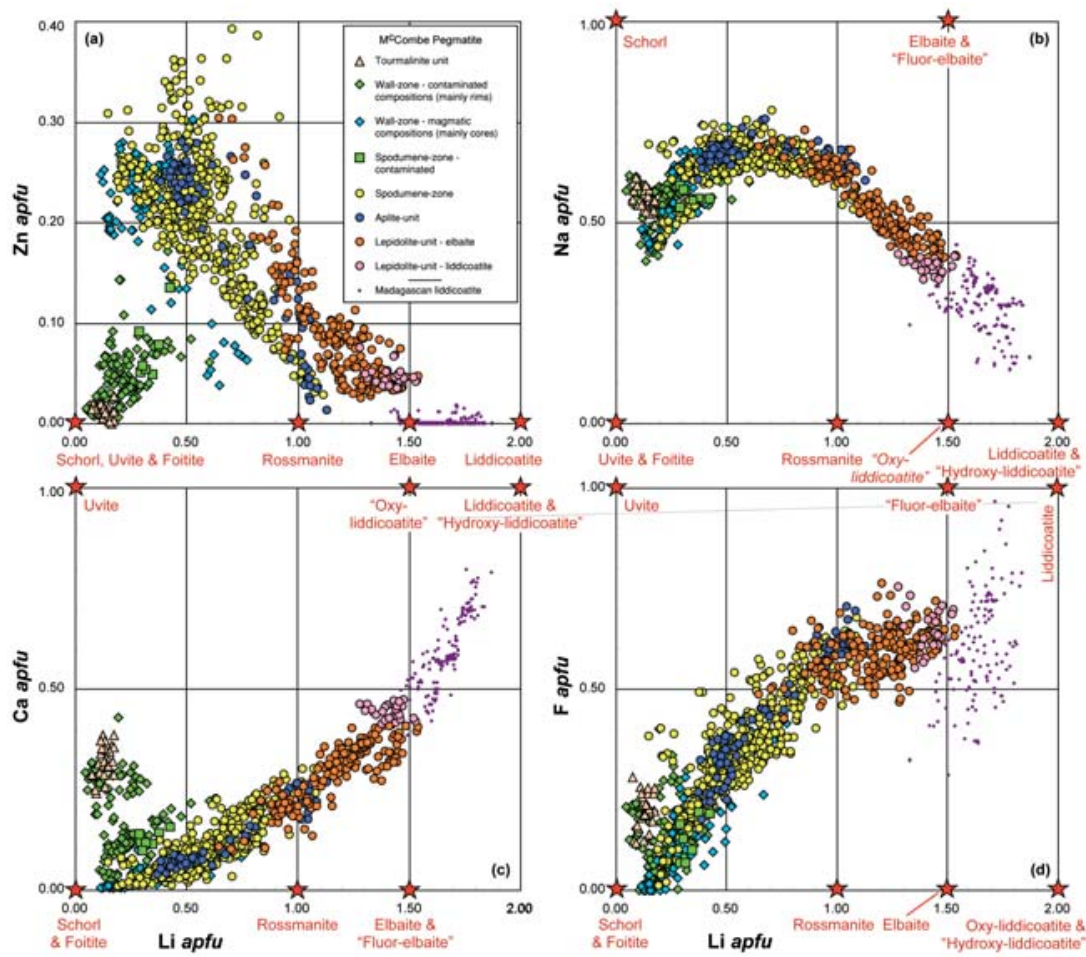


Fig. 9. Covariation of Li with X-, Y- and W-site cations in tourmaline from the McCombe pegmatite, compared with selected data on liddicoatite from Madagascar (Dirlam *et al.* 2002; A.G. Tindle, unpubl. data). (a) Li versus Zn (apfu). (b) Li versus Na (apfu). (c) Li versus Ca (apfu). (d) Li versus F (apfu).

Formation of the spodumene zone continued long after the wall zone had solidified.

5. During event 4, there is a sudden drop in pressure within the pegmatite and a rapid quench of the remaining pegmatite-forming melt occurred. The aplite unit thus formed and crystallized tourmaline with very similar compositions to that in the spodumene zone.

6. Within the mainly crystallized spodumene zone and aplite unit, trapped pockets of evolved "melt" developed and gave rise to the most evolved product of fractional crystallization, the lepidolite unit, host to the tourmaline species "fluor-elbaite" and liddicoatite. The offset in Zn data from lepidolite-unit tourmaline (Fig. 9a) and the marked drop in Mg + Ti at 0.7 apfu

Fe²⁺ (Fig. 10) indicate some perturbation of the fractionation scheme at this point, perhaps through a transition from melt-dominated to fluid-dominated crystallization.

In conclusion, the McCombe pegmatite appears to have crystallized from a pegmatite-forming melt that interacted with Ca-, Mg-, and Ti-rich host-rocks, became contaminated *in situ*, and through prolonged fractionation of this contaminated melt, aided by Ca-F complexing, was able to crystallize liddicoatite. It is likely a rare beast because of what it was contaminated with, rather than because it evolved from an unusual magma.

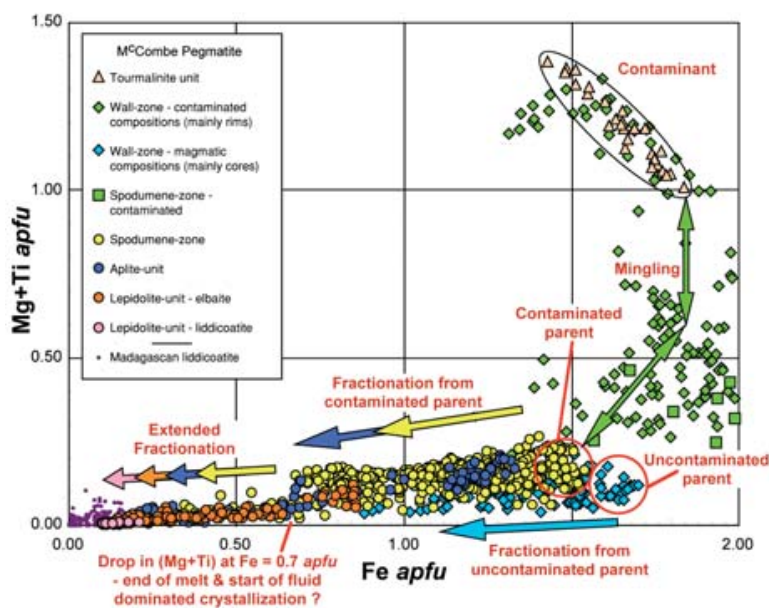


FIG. 10. Covariation of Fe versus Mg + Ti in tourmaline, with indications of some of the processes and interactions that occurred during the crystallization interval of the McCombe pegmatite.

ACKNOWLEDGEMENTS

Michelle Higgins, Kay Green, Brian Ellis, John Watson and Carole-Anne MacDonald helped with sample preparation, including the preparation of many polished thin sections and blocks for electron-microprobe analysis. AGT thanks the Ontario Geological Survey for support in the field, and Richard Tayler for providing a specimen of Madagascar liddicoatite. We also thank Petr Černý, Fuat Yavuz and Peter Webb for constructive comments, and Robert F. Martin for his editorial work. This contribution is published with the permission of the Senior Manager, Precambrian Geoscience Section of the Ontario Geological Survey.

REFERENCES

- AKIZUKI, M., KURIBAYASHI, T., NAGASE, T. & KITIKAZE, A. (2001): Triclinic liddicoatite and elbaite in growth sectors of tourmaline from Madagascar. *Am. Mineral.* **86**, 364-369.
- AURISICCHIO, C., DEMARTIN, F., OTTOLINI, L. & PEZZOTTA, F. (1999): Homogeneous liddicoatite from Madagascar: a possible reference material? First EMPA, SIMS and SREF data. *Eur. J. Mineral.* **11**, 263-280.
- BASTOS, F.M. (2002): The Barra de Salinas pegmatites, Minas Gerais, Brazil. *Mineral. Rec.* **33**, 209-216.
- BREAKS, F.W. & BOND, W.D. (1993): The English River Subprovince – an Archean gneissic belt: geology, geochemistry and associated mineralization. *Ontario Geol. Surv., Open File Rep.* **5846**.
- _____, SELWAY, J.B. & TINDLE, A.G. (2001): Project Unit 01–304. Fertile peraluminous granites and related rare-element pegmatite mineralization, Superior Province, northwest and northeast Ontario. In *Summary of Field Work and Other Activities 2001*. *Ontario Geol. Surv., Open File Rep.* **6070**, 39-1 – 39-39.
- _____, _____ & _____ (2003): Fertile peraluminous granites and related rare-element mineralization in pegmatites, Superior Province, northwest and northeast Ontario. *Ontario Geol. Surv., Open File Rep.* **6099**.
- _____, & TINDLE, A.G. (2002): Rare-element mineralization of the Separation Lake area, northwest Ontario: characteristics of a new discovery of complex-type, petalite-subtype, Li–Rb–Cs–Ta pegmatite. In *Industrial Minerals in Canada* (S. Dunlop & G.J. Simandl, eds.). *Can. Inst. Mining, Metall. & Petroleum, Spec. Vol.* **53**, 159-178.
- BURNS, P.C., MACDONALD, D.J. & HAWTHORNE, F.C. (1994): The crystal chemistry of manganese-bearing elbaite. *Can. Mineral.* **32**, 31-41.
- BURT, D.M. (1982): Minerals of beryllium. In *Granitic Pegmatites in Science and Industry* (P. Černý, ed.). *Mineral. Assoc. Can., Short-Course Handbook* **8**, 135-148.

- ČERNÝ, P. (1991): Rare-element granitic pegmatites. 1. Anatomy and internal evolution of pegmatite deposits. *Geosci. Can.* **18**, 49-67.
- _____, ERCIT, T.S., TRUEMAN, D.L., GOAD, B.E. & PAUL, B.J. (1981): The Cat Lake – Winnipeg River and Wekusko Lake pegmatite fields, Manitoba. *Manitoba Dep. Energy and Mines, Mineral Resource Div., Econ. Geol. Rep. ER80-1*.
- _____, _____, & VANSTONE, P.T. (1998): Mineralogy and petrology of the Tanco rare- element pegmatite deposit, southeastern Manitoba. *Int. Mineral. Assoc., 17th Gen. Meeting (Toronto), Field Trip B6*.
- _____ & HAWTHORNE, F.C. (1982): Selected peraluminous minerals. In *Granitic Pegmatites in Science and Industry* (P. Černý, ed.). *Mineral. Assoc. Can., Short-Course Handbook* **8**, 163-186.
- _____ & MACEK, J. (1972): The Tanco pegmatite at Bernic Lake, Manitoba. Coloured potassium feldspars. *Can. Mineral.* **11**, 679-689.
- _____ & SIMPSON, F.M. (1977): The Tanco pegmatite at Bernic Lake, Manitoba. IX. Beryl. *Can. Mineral.* **15**, 489-499.
- DIRLAM, D.M., LAURS, B.M., PEZZOTTA, F. & SIMMONS, W.B. (2002): Liddicoatite tourmaline from Anjanaboina, Madagascar. *Gems & Gemology* **38**, 28-53.
- DUNN, P.J., APPLEMAN, D.E. & NELEN, J.E. (1977): Liddicoatite, a new calcium end-member of the tourmaline group. *Am. Mineral.* **62**, 1121-1124.
- ERCIT, T.S., GROAT, L.A. & GAULT, R.A. (2003): Granitic pegmatites of the O'Grady batholith, N.W.T., Canada: a case study of the evolution of the elbaite subtype of rare-element granitic pegmatite. *Can. Mineral.* **41**, 117-137.
- FORTEY, N.J., COATS, J.S., GALLAGHER, M.J., SMITH, C.G. & GREENWOOD, P.G. (1993): New strata-bound barite and base metals in Middle Dalradian rocks near Braemar, north-east Scotland. *Trans. Inst. Mining Metall. (Sect. B: Appl. Earth Sci.)* **102**, 55-64.
- _____, NANCARROW, P.H.A. & GALLAGHER, M.J. (1991): Armenite from the Middle Dalradian of Scotland. *Mineral. Mag.* **55**, 135-138.
- HAWTHORNE, F.C. & HENRY, D.J. (1999): Classification of the minerals of the tourmaline group. *Eur. J. Mineral.* **11**, 201-215.
- HOFFMAN, H.J. (1985): Archean stromatolites from Uchi greenstone belt, northwestern Ontario. In *Evolution of Archean Supracrustal Sequences. Geol. Assoc. Can., Spec. Pap.* **28**, 125-132.
- JOLLIFF, B.L., PAPIKE, J.J. & SHEARER, C.K. (1986): Tourmaline as a recorder of pegmatite evolution: Bob Ingersoll pegmatite, Black Hills, South Dakota. *Am. Mineral.* **71**, 422-500.
- _____, _____ & _____ (1987): Fractionation trends in mica and tourmaline as indicators of pegmatite internal evolution: Bob Ingersoll pegmatite, Black Hills, South Dakota. *Geochim. Cosmochim. Acta* **51**, 519-534.
- LAURS, B.M., DILLES, J.H., WAIRRACH, Y., KAUSAR, A.B. & SNEE, L.W. (1998): Geological setting and petrogenesis of symmetrically zoned, miarolitic granitic pegmatites at Stak Nala, Nanga Parbat – Haramosh Massif, northern Pakistan. *Can. Mineral.* **36**, 1-47.
- MACDONALD, D.J., HAWTHORNE, F.C. & GRICE, J.D. (1993): Foitite, $\square[\text{Fe}^{2+}_2(\text{Al,Fe}^{3+})\text{Al}_6\text{Si}_6\text{O}_{18}(\text{BO}_3)_3(\text{OH})_4$, a new alkali-deficient tourmaline: description and crystal structure. *Am. Mineral.* **78**, 1299-1303.
- MORGAN, G.B., VI & LONDON, D. (1987): Alteration of amphibolitic wallrocks around the Tanco rare-element pegmatite, Bernic Lake, Manitoba. *Am. Mineral.* **72**, 1097-1121.
- MULLIGAN, R. (1965): Geology of Canadian lithium deposits. *Geol. Surv. Can., Econ. Geol. Rep.* **21**.
- NOVÁK, M. (2000): Compositional pathways of tourmaline evolution during primary (magmatic) crystallization in complex (Li) pegmatites of the Moldanubicum, Czech Republic. In *Mineralogy and Petrology of Shallow Depth Pegmatites* (F. Pezzotta, ed.). *Memorie della Società Italiana di Scienze Naturali e del Museo Civico di Storia Naturale di Milano* **XXX(I)**, 45-56.
- _____ & POVONDRA, P. (1995): Elbaite pegmatites in the Moldanubicum: a new subtype of the rare-element class. *Mineral. Petrol.* **55**, 159-176.
- _____ & SELWAY, J.B. (1997): Tourmaline composition as a recorder of crystallization in open and closed systems in the elbaite-subtype pegmatite from Blizná. In *Tourmaline 1997 Symp. (Nové Mesto na Morave)*, Abstr. Vol., 62-63.
- _____, _____, ČERNÝ, P., HAWTHORNE, F.C. & OTTOLINI, L. (1999): Tourmaline of the elbaite–dravite series from an elbaite-subtype pegmatite at Blizná, southern Bohemia, Czech Republic. *Eur. J. Mineral.* **11**, 557-568.
- POUCHOU, J.L. & PICOIR, F. (1985): "PAP" procedure for improved quantitative analysis. *Microbeam Anal.* **20**, 104-105.
- PYE, E.G. (1956): Lithium in northern Ontario. *Can. Mining J.* **77**, 73-75.
- RINALDI, R., ČERNÝ, P. & FERGUSON, R.B. (1972): The Tanco pegmatite at Bernic Lake, Manitoba. VI. Lithium rubidium cesium micas. *Can. Mineral.* **11**, 690-707.
- ROBERT, J.-L., GOURANT, J.-P., LINNEN, R.L., ROUER, O. & BENOIST, P. (1997): Crystal-chemical relationships between OH, F and Na in tourmaline. In *Tourmaline 1997 Symp. (Nové Mesto na Morave)*, Abstr. Vol., 84-85.
- SAHAMA, T.G., VON KNORRING, O. & TÖRNROOS, R. (1979): On tourmaline. *Lithos*, **12**, 109-114.

- SELWAY, J.B., ČERNÝ, P. & HAWTHORNE, F.C. (2000): The Tanco pegmatite at Bernic Lake, Manitoba. XIV. Internal tourmaline. *Can. Mineral.* **38**, 877-891.
- _____, NOVÁK, M., ČERNÝ, P. & HAWTHORNE, F.C. (1999): Compositional evolution of tourmaline in lepidolite-subtype pegmatites. *Eur. J. Mineral.* **11**, 569-584.
- _____, SMEDS, S.-A., ČERNÝ, P. & HAWTHORNE, F.C. (2002): Compositional evolution of tourmaline in the petalite-subtype Nyköpingsgruvan pegmatites, Utö, Stockholm archipelago, Sweden. *GFF* **124**, 93-102.
- TEERTSTRA, D.K., ČERNÝ, P. & HAWTHORNE, F.C. (1998): Rubidium feldspars in granitic pegmatites. *Can. Mineral.* **36**, 483-496.
- _____, _____ & OTTOLINI, L. (1999a): Stranger in paradise: liddicoatite from the High Grade Dyke pegmatite, southeastern Manitoba, Canada. *Eur. J. Mineral.* **11**, 227-235.
- _____, _____ & _____ (1999b): Geochemistry and petrology of late K- and Rb-feldspars in the Rubellite pegmatite, Lilypad Lakes, NW Ontario. *Mineral. Petrol.* **65**, 237-247.
- THURSTON, P.C. (1985a): Geology of the Earngey-Costello area, District of Kenora, Patricia Portion. *Ontario Geol. Surv., Geol. Rep.* **234**.
- _____. (1985b): Physical volcanology and stratigraphy of the Confederation Lake area, District of Kenora (Patricia Portion). *Ontario Geol. Surv., Rep.* **236**.
- TINDLE, A.G., BREAKS, F.W., SELWAY, J. B. (2001): Electron microprobe compositions of tantalum-bearing oxides and potassium feldspar from rare-element granitic pegmatites, Superior Province, northwestern Ontario. *Ontario Geol. Surv., Misc. Release – Data* **90**.
- _____, _____ & _____ (2002b): Tourmaline in petalite-subtype granitic pegmatites: evidence of fractionation and contamination from the Pakeagama Lake and Separation Lake areas of northwestern Ontario, Canada. *Can. Mineral.* **40**, 753-788.
- _____, SELWAY, J.B. & BREAKS, F.W. (2002a): Electron microprobe and bulk analyses of fertile peraluminous granites and related rare-element pegmatites, Superior Province, Northwest and Northeast Ontario. *In Operation Treasure Hunt. Ontario Geol. Surv., Misc. Release—Data* **111**, chemical analyses to accompany *Open-File Rep.* **6099**.
- _____. & WEBB, P.C. (1990): Estimation of lithium contents in trioctahedral micas using microprobe data: application to micas from granitic rocks. *Eur. J. Mineral.* **2**, 595-610.
- WALLACE, H. (1978): Geology of the Opik eigen Lake area, District of Thunder Bay. *Ontario Geol. Surv., Rep.* **185**.
- WEIDNER, J.R. & MARTIN, R.F. (1987): Phase equilibria of a fluorine-rich leucogranite from the St. Austell pluton, Cornwall. *Geochim. Cosmochim. Acta* **51**, 1591-1597.
- ZAGORSKIY, V.E., PERETYAZHKO, I.S., SCHIRYEVNA, V.A. & BOGDANOVA, L.A. (1989): Tourmalines from miarolitic pegmatites in the Malkhan Range (Transbaikalia). *Mineral. Zh.* **11**, 44-55 (in Russ.).

Received February 20, 2004, revised manuscript accepted January 3, 2005.